Numerical Simulation of the Motion of Granular Material

A. Džiugys, B. Peters
Institut für Angewandte Thermo- und Fluiddynamik

Forschungszentrum Karlsruhe

Technik und Umwelt

Wissenschaftliche Berichte

FZKA 6156

Numerical Simulation of the Motion of Granular Material

A. Džiugys*
B. Peters

Institut für Angewandte Thermo- und Fluiddynamik

*Lithuanian Energy Institute, Kaunas, Lithuania

ABSTRACT

Technical applications involving a packed bed of particles are frequently used in the processing industry, energy-supplying industry and in waste incineration plants. Common to all these applications is that the entire flow and combustion process consists of several important thermodynamic and fluid dynamic processes, among which are the motion of the packed bed with its redistribution of particles and the chemical conversion processes of heterogeneous combustion. The objective of this report is to present a numerical simulation method to model the motion of the packed bed on a moving grate or in a rotary kiln. The packed bed can be described as granular material consisting of a large number of particles.

A short review of the presently feasible major methods of numerical simulation of the motion of granular material shall be given in the report.

The method chosen is the Lagrangian time-driven method and it uses the position, the orientation, the velocity and the angular velocity of particles as independent variables. These are obtained by time integration of the three-dimensional dynamics equations which were derived from the classical Newtonian mechanics approach based on the second law of Newton for the translation and rotation of each particle in the granular material. This includes the keeping track of all forces and moments acting on each particle at every time step. Particles are treated as contacting elastic bodies which can overlap each other. Contact forces depend on the overlap geometry, material properties and dynamics of particles. Contact forces include normal and tangential components of repulsion force with visco-elastic models for energy dissipation and friction. A detailed review of possible models of a time-driven method is presented in the report.

The simulation method is based on Object Oriented Programming methodologies and programmed in the programming language C++. This approach supports objects which can be used for three dimensional particles of various shapes and sizes and for walls as boundaries. The programming code is implemented in the TOSCA software package (Tools of Object-oriented Software for Continuum Mechanic Applications) which allows for a high degree of flexibility and for shortening the duration of the software development process.

As methods for particle motion may deal with particles of different sizes and materials, the approach allows to describe conversion processes in technical applications.

After describing the simulation method results of test cases of particle motion in boxes and rotary kiln are presented. The equations of particle motion were solved by the Gear predictor-corrector scheme of 5th order accuracy. The results indicate that a major problem to simulate the motion on a grate has been solved.

NUMERISCHE SIMULATION DER BEWEGUNG GRANULARER MEDIEN

ZUSAMMENFASSUNG

Festbetten bestehend aus granularen Materialien sind häufig in der verfahrenstechnischen, der energieversorgenden Industrie oder bei der Müllverbrennung zu finden. All diesen Anwendungen ist gemeinsam, daß sich der gesamte chemische Prozeß aus verschiedenen thermodynamischen und strömungsmechanischen Prozessen zusammensetzt, zu denen die Bewegung des Festbettes und die chemische Umwandlung der Partikel im Festbett gehört. Das Ziel dieses Berichts besteht darin, eine numerische Simulationsmethode für die Festbettbewegung auf dem Rost oder im Drehrohr zu identifizieren. Dabei wird das Festbett als ein granulares Material mit einer endlichen Anzahl von Einzelpartikeln betrachtet.

Eine Übersicht der zur Zeit hauptsächlich verwendeten numerischen Methoden zur Simulation der Festbettbewegung wird im Bericht vorgestellt.

Die für die Simulation gewählte Methode beruht auf dem Lagrange-Ansatz und beinhaltet die Position, die Orientierung, die Rotation und die Geschwindigkeit der Partikel als unabhängige Variablen. Sie werden aus der Integration der dreidimensionalen Newtonschen Bewegungsgleichungen, angewendet auf jedes Partikel des Festbettes, erhalten. Dabei werden die Partikel als elastisch angesehen, die miteinander kollidieren können, was durch eine entsprechende Überlappung repräsentiert wird. Dabei hängt die Kontaktkraft von der Überlappung, den Materialeigenschaften und der Dynamik ab. Die Kontaktkräfte setzen sich aus Normal- und Tangentialkomponenten an der Kontaktstelle mit dissipativen Effekten zusammen.

Die Simulationsmethode basiert auf der objekt-orientierten Programmiertechnik und ist in C++ geschrieben. Dieser Ansatz unterstützt Objekte, die sowohl Partikel verschiedener Größe und Form als auch Wände wiedergeben können. Die Methoden sind in TOSCA (Tools of Object-oriented Software for Continuum Mechanic Applications) eingebettet, was einen hohen Grad an Flexibilität und verkürzte Entwicklungszeiten garantiert.

Nach der Beschreibung der Simulationsmethode werden verschiedene Testfälle für die Bewegung der Partikel in geschlossenen Behältern und im Drehrohr vorgestellt. Die Bewegungsgleichungen werden mit einem Prädiktor-Korrektor Schema (5. Ordnung) von Gear gelöst. Die Ergebnisse zeigen, daß die Methode für die Beschreibung der Bewegung von Festbetten auf dem Rost und im Drehrohr geeignet ist, und damit ein wesentlichen Teilproblem innerhalb des Komplexes der Müllverbrennung gelöst ist.

Contents

ABBREVIATIONS

BD4   Backwards Differentiation Scheme of Fourth Order (page 55)

CMM   Continuum Mechanics Method (page 5)

DEM   Discrete (or Distinct) Elements Method (page 5)

DMT   Model of Derjaguin, Muller and Toporov (page 35)

EDM   Event-Driven Method (page 7)

GM   Granular Material (page 1)

JKR   Model of Johnson, Kendall and Roberts (page 35)

MD   Molecular Dynamics (page 7)

NSA   Neighbors-Search Algorithm (page 59)

OOP   Object-Oriented Programming Methodology (page 57)

PBC   Periodic Boundary Condition (page 23)

RK4   Runge-Kutta Scheme of Fourth Order (page 55)

TDM   Time-Driven Method (page 8)

TOSCA Tools of Object-oriented Software for Continuum mechanic Applications (page 58)

I. INTRODUCTION
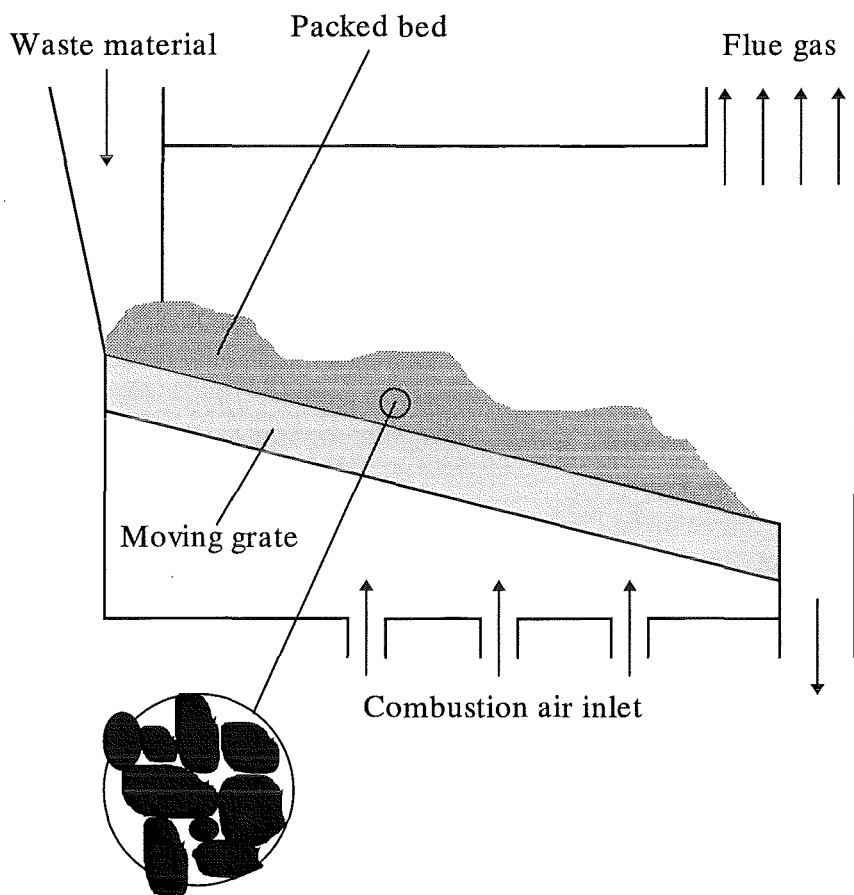
Figure 1. Burning of waste in a packed bed

Technical applications involving a packed bed of particles are frequently used in the processing industry, energy-supplying industry and in waste incineration plants. Common to all these applications is that the entire flow and combustion process consists of several important thermodynamic and fluid dynamic processes, among which are the motion of the packed bed with its redistribution of particles and the chemical conversion processes of heterogeneous combustion. The packed bed can be described as granular material (GM) which can be idealised as an ensemble of a large number of particles.

In general, the motion of particles of various size, shape and material in the turbulent flow is restricted by walls of various configuration. Ideally, the interaction between the turbulent motion of the surrounding fluid and the particles has to be taken into account to achieve a high degree of accuracy. At the same time, collision dynamics of the particles must be solved as for elastic bodies consisting of molecules. However, this problem is too complex for the computers available and, on the other hand, such a high accuracy is not needed today. Hence, the main problem can be reduced by dividing it into several sub-problems (Figure 1):

1. pure fluid dynamics apply to areas without any particles in the fluid (area of combustion air inlet in Figure 1).

2. In region such as above the packed bed in the flue gas where the particles are too small, the motion of such particles can be solved as a transport of a scalar quantity in the fluid. However, for large particles, without the need to separate particles and fluid, this suspension can be modelled as an additional phase.

3. In areas where the influence of the fluid is negligible, the behaviour of granular material only can be simulated (supply of waste into the combustion chamber).

4. In areas where the interaction between the particles and the fluid is important, the simulation of the system can be divided into two separate simulations

    a) Motion of fluid: The fluid motion through granular media is modelled by a flow through porous material according to the properties of granular material.

    b) Motion of granular material: It corresponds to the same as problem 3, with additional drag and buoyancy forces of the fluid influencing the granular material.

Under these assumptions, problems 1, 2 and 4a can be solved accurately by methods and models of fluid dynamics. Problems 3 and 4b describe the problem of granular material behaviour with the interaction between fluid and particles as an additional force. In general, the walls of a furnace act as bounding surface for the fluid and the packed bed and radiate both into the gas and onto the surface of a packed bed.

At this stage, our main tasks include

- To analyse possibilities of simulating the behaviour of granular material in combination with a simulation of fluid dynamics.

- To develop a software module to simulate the motion of granular material. The module must be implemented in the software package **TOSCA** (Tools of Object-oriented Software for Continuum Mechanics Applications) (Peters (1996), Peters (1997)).

- To simulate some testing problems of granular material motion.

The present report contains

- a short review of granular material phenomena

- a short review of the main methods to simulate the motion of granular material

- an extended literature survey and a detailed description of the method used

- and the results of simulated test cases.

II. SHORT REVIEW OF GRANULAR MATERIAL PHENOMENA

The following review was carried out with regard to the motion of waste material on a moving gate. Chemical processes of waste combustion in a packed bed are defined by particles-fluid and particle-particle interactions. Therefore, the understanding of the motion of waste material in a packed bed would be very useful for the handling of combustion processes. However, various kind of granular materials exist. Fields of application of granular material include: Chemical industry with particulate reaction engineering (Fan *et al.* (1994)); design of powders and grain flows and storage; separation; granulation etc. Therefore, the handling of granular material is of particular interest for industry. For example, at least 40% (~61 billion US dollars) of all money investments of the US chemical industry in 1993 were spent in particle technology (Ennis *et al.* (1994)).

Granular materials are simple systems of a large number of particles of various size, shape and material and can be classified in accordance with particle size (Table 1). The motion of each particle is defined by classical Newtonian mechanics and contact mechanics of deformation. Although this seems to be simple, the properties and phenomena of granular material are far away from being understood completely. The reason is that the dynamics of granular material is highly dissipative, i.e. the time scale of energy dissipation is less than the time needed to equilibrate the granular material spatially and the particle size is large as compared to the length scale of flow variation (Umbanhowar (1997)).

Particle size range	Material	Individual component
0.1 μm - 1.0 μm	Ultra-fine powder	Ultra-fine particle
1.0 μm - 10 μm	Super-fine powder	Super-fine particle
10 μm - 100 μm	Granular powder	Granular particle
100 μm - 3.0 mm	Granular solid	Granule
3.0 mm - 10mm	Broken solid	Grain

Table 1. Types of granular material (according to Nedderman (1992))

For example, a major property of granular material is the packing density which is defined as the volume fraction of the granular made up by solids. The packing density is very important in science, soil mechanics, industry, ceramics and concrete production etc. Manufacturing processes involving the handling of powders were estimated to reach rarely more than 60% of their designed capacity in 1994 (Ennis *et al.* (1994), Knowlton *et al.* (1994)). Porosity of granular material, which is important for our simulations, is defined by the packing density and is very significant for processes of waste combustion. Stoval *et al.* (1986) proposed a linear model of packing density according to the size of particles. But such kind of model has restrictions, because the packing density depends on the history of granular material motion and it may vary at the different granular material locations. It is widely known that particles

3

may form arches that affect to the packing (for example Luding *et al.* (1996)). Akiyama *et al.* (1996) demonstrated by experiment and simulation that convective motions and the mixing of particles within vertically vibrating particle beds may exhibit a fractal property.

The behaviour of granular material is determined by the nature of the contact between the particles, i.e. by material and geometrical properties of the particles. Depending on the conditions prevailing, however, the granular material may demonstrate various properties and behaviours with various states of material. Granular material can be deformed as solid bodies or soils, it may have a flowability corresponding to that of liquids and a compressibility like that of gases.

For example:

- Granular material may form shear layers under the influence of shear forces. Recently, it was found that frictional forces between two layers may exhibit a hysteresis depending on the velocity of layers (Nasuno *et al.* (1997), Lubkin (1997)). Solitons were found in the investigations of the cooperative behaviour of particles (Umbanhowar *et al.* (1996), Umbanhowar (1997), Shinbrot (1997)).

- Groups of solid particles wetted by viscous liquid form agglomerates in the dry granular material. Such wet agglomerates often occur in a stationary or flowing powders and are more stable under shear then similar dry agglomerates. This phenomenon was investigated in details by Khan and Tardos (1997).

Descriptions and investigations of many other problems, phenomena and properties of granular material can be found for example in Jaeger, Liu and Nagel (1989), Campbell (1990), Jaeger and Nagel (1992), Rietema (1991), Nedderman (1992), Bridgwater (1993), Behringer and Baxter (1993), Ristow (1994b), Ennis *et al.* (1994), Knowlton *et al.* (1994), Fan *et al.* (1994), Jaeger *et al.* (1996), McNamara and Young (1996), Herrmann (1997), Jaeger and Nagel (1997), Umbanhowar (1997) *etc.*

4

III. MAJOR METHODS TO SIMULATE THE MOTION OF GRANULAR MATERIAL

As above-mentioned, granular materials may be deformed as solid bodies or soils, they may be flowable as liquids or as compressible as gases. With respect to the tasks and accuracy required, various methods may be used to simulate the motion of granular material. However, it is difficult to classify all methods by one strict scheme. According to Hogue and Newland (1994) the methods to simulate the behaviour of granular material may be classified by two approaches:

- continuum mechanics methods (CMM) or macroscopic modelling

- discrete (or distinct) elements methods (DEM) or microscopic (particle-level) modelling

III.1 CONTINUUM MECHANICS APPROACH

The method of continuum mechanics can be used for the simulation of the motion of granular material with the latter being described as a continuum media, such as:

- viscous-plastic "granular fluid"

- "granular gases" with a set of continuum equations derived from microscopic models of individual particle interactions (Campbell (1990)

- viscous-elastic-plastic soil

In this case, it is possible to use equations of continuum mechanics (e.g. fluid dynamics) as a basis for the creation of mathematical models. Nevertheless, suitable mathematical models for the description of such complex and unexplained phenomenon of various granular material are still lacking, due to the large range of material and particle shapes, features of cooperative motion and structures (e.g. state of "granular solid") and energy dissipation in inelastic collisions of particle-particle and wall-particle. Therefore, usual processes of granular material motion may yield results that are unexplainable from the continuum mechanics point of view (e.g. dissipation of energy is necessary for soliton structures (Fineberg (1996), Umbanhowar et al. (1996)).

Models of CMM involve equations for a two-phase turbulent flow and are usually complex to solve. They can be applied to particular materials and particular processes only (Barker (1993)). On the other hand, the results of CMM may differ from the experimental data by up to an order of magnitude (Savage (1988)). More or less suitable models only exist for spherical particles.

Descriptions and reviews of CMM are widely available (e.g. Runesson et al. (1986), Polderman et al. (1987), Johnson and Jackson (1987), Savage (1988), Campbell (1990), Gu et al. (1992), Adams and Briscoe (1993), Abu-Zaid and Ahmadi (1993)). Most of them use the Eulerian approach for the granular material behaviour.

5

The interesting and elegant simple random map model which was proposed by Metcalfe *et al.* (1995) is based on the Lagrangian approach of CMM. Assuming a rotating drum that is partially filled with granular material (Figure 2), an avalanche occurs when the surface slope of the granular material exceeds the critical value $\theta_{avalanche}$. After the avalanche ceases, the surface returns to its angle of repose θ_{repose}. The avalanche transports an initial wedge of material downhill to the new wedge. After some rotation of the drum, this new wedge will be divided into several parts by the intersection of following wedges and, thus, the granular media will be mixed. As shown, it is possible to predict the mixing behaviour to a surprising degree of accuracy.
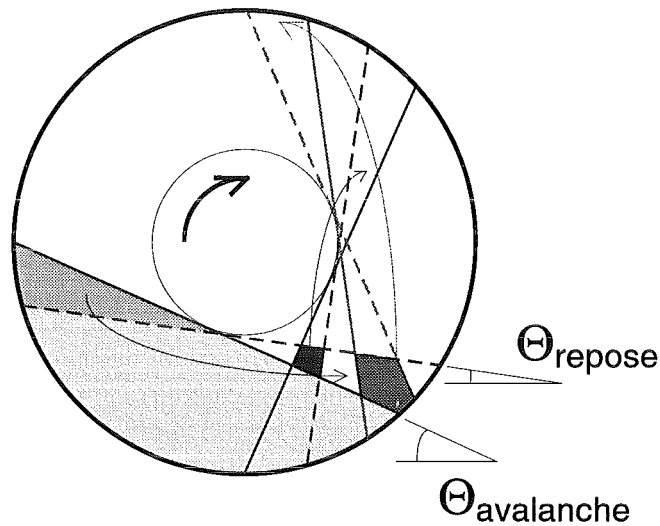
Figure 2. Random map method (according to Metcalfe *et al.* (1995))

III.2 DISCRETE ELEMENTS APPROACH

The discrete elements methods (DEM) is simple, because it is fully based on the Lagrangian approach for the simulation of motion of GM on the microscopic level of particles. This means that the DEM can be used to calculate quantities that are difficult to obtain experimentally and at the same time it can be used to improve CMM. DEM is applicable for simulations of molecular dynamics (MD) too. Therefore, methods to simulate granular material and MD shall be reviewed here. The DEM's can be divided into three main classes:

- Statistical mechanics models

- Classical Newtonian dynamics models

- Hybrid models

STATISTICAL MECHANICS MODELS use stochastic components in the particle displacements, for example, the Monte Carlo method(Perram *et al.* (1984), Rosato *et al.* (1987), Devillard (1990), Camp and Allen (1996)), the *cellular automata* method (Baxter and Behringer (1990)), or the *random walk* approach (Caram and Hong (1991)).

CLASSICAL NEWTONIAN DYNAMICS MODELS use equations of particle dynamics derived from classical Newtonian mechanics for each particle. These methods can be divided into two major groups:

- Event-driven methods (EDM);

- Time-driven methods (TDM).

The *Event-driven method* (EDM) is based on instantaneous collisions, which means that the state of the particles is updated only at the times of the events i.e. collisions of the particles. The paths of particles are calculated by the equations of momentum, angular momentum and energy. Free motion of particles that are no in contact with each other is described by equations of forces acting on the particles. Sometimes this method is also referred to as hard spheres method. Energy dissipation of collisions is defined by the coefficient of restitution, which can be set according to Newton's law of restitution or Poisson's hypothesis.

However, the principle of energy conservation may be violated under certain conditions by Newton's law and Poisson's hypothesis (Hogue and Newland (1994)). A more accurate description of the dissipation of energy is achieved by the theories of Brach (1984), Keller (1986), Kuwabara and Kono (1987), Brach (1989), Stronge (1990), Wang and Mason (1992), Hogue and Newland (1994), Kumaran (1997)). For molecular dynamics, energy dissipation on the collisions is zero.

All collisions between particles are assumed to be binary and quasi-instantaneous. Contacts occur at a point only with impulsive interaction forces and negligible other forces during collision. Equations of momentum and angular momentum describe the changes of momentum and angular momentum between the colliding particles and of the free motion of particles that are not in contact with each other. The event-driven method is suitable when the particles collide asynchronously and the time between the events is smaller than the real time of collisions between real particles would be. EDM was successfully applied in numerous

7

simulations of granular material and molecular dynamics (*e.g.* Rapaport (1980), Allen *et al.* (1989), Lubachevsky (1991), McNamara and Young (1994), Luding *et al.* (1996), Hoomans *et al.* (1996), Marin (1997)).

Peters (1994) applied EDM for non-equilibrium molecular dynamics, where inter-molecule interactions were not calculated, and only collisions of large objects with molecules were calculated.

When the time of collision between real particles is larger than the time of the free path of particles, then a *time-driven method* (TDM) is better suited. Here, the current state of all particles, at the time t, are updated after fixed time step Δt, which is smaller than the smallest time of impacts. The state of particles is obtained by time integration of the three-dimensional dynamics equations derived from the classical Newtonian mechanics approach based on the Newton's second law for translation and rotation of each particle in the granular material. This includes the keeping track of all the forces and moments acting on each particle at every time step. Particles are treated as contacting elastic bodies which can overlap each other. Contact forces depend on the overlap geometry, material properties and dynamics of the particles. Contact forces include both the normal and tangential components of the repulsion force with visco-elastic models for energy dissipation and friction. A detailed review of possible models of the time-driven method is presented in the report below.

HYBRID MODELS. Hogue and Newland (1994) describe a contact model which combines ideas from statistical mechanics and classical Newtonian dynamics models. The motion of particles is simulated by an event driven method with using pseudo-random coefficients of restitution for energy dissipation.

III.3 OTHER APPROACHES

Other interesting approaches include the

- Geometrical *steepest descent* method (Jullien and Meankin (1987), Meankin and Jullien (1992));

- *Shinbrot's model* (Shinbrot (1997)) which is combination of CMM and DEM approaches (Umbanhowar (1997));

- *Quasi-static* approach described and used by Borja and Wren (1995) and Wren and Borja (1997).

III.4 CONCLUSIONS

The requirements to choose a method to simulate the motion of granular material are

- Granular material consists of particles of various sizes and materials

- Full information about position and motion of each particle

- Coupling between particles and fluid flow

- Detailed description of particle-fluid interaction and inner-particle chemical processes

It means that a resolution up to single particle is necessary. Only methods based on *classical Newtonian dynamics models* of DEM can satisfy such requirements. In the packed bed, particles are almost always in contact with neighbours. Therefore, the *time-driven method* was chosen for simulations of the motion of waste material in a packed bed. The time-driven method shall be reviewed in more detail below.

IV. TIME-DRIVEN METHOD FOR ELASTIC PARTICLES

IV.1 INTRODUCTION

The time-driven method is based on the original method proposed by Cundal and Strack (1979) for the contact-force model of discrete element dynamics. The method chosen bases itself on a Lagrangian frame of reference which takes the particles position, orientation, translational and angular velocity as independent variables. They are obtained by an integration of a system of fully deterministic classical Newtonian dynamics equations for each particle. For this purpose, explicit expressions for all forces acting on and between the particles have to be evaluated. Particles in contact are deformed in reality (Figure 3). But it is assumed that the visco-elastic impact between the particles can be described as one particle shape overlapping another one with the contact forces between them depending on the overlap geometry, the material of the particles, and the relative velocity of the particles in the contact area.

real deformation of particles

h_{ij}

particle deformation as overlap
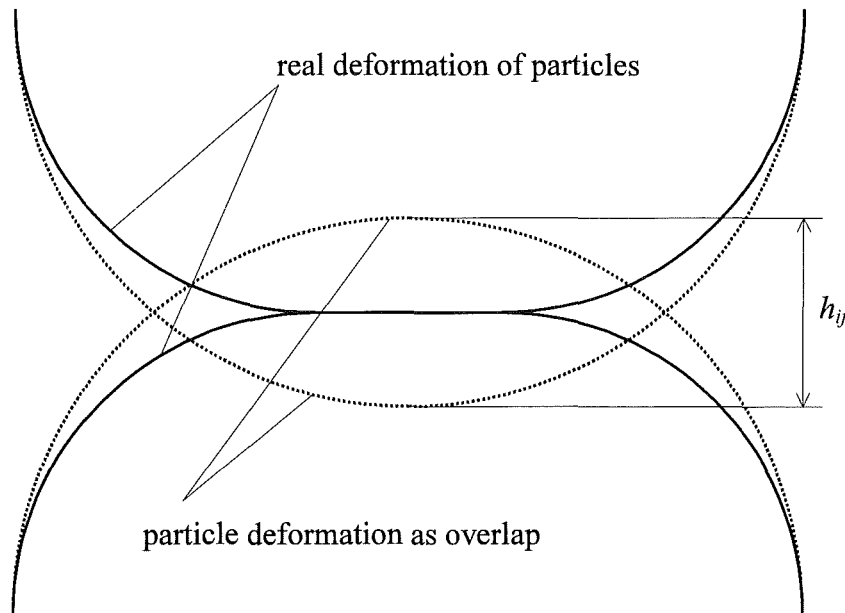
Figure 3. Elastic contact of two particles as overlap

In the numerical simulation, velocities and accelerations are assumed to be constant during current time step. For such a method disturbances resulting from particle collisions propagate to neighbour particles only.

IV.1.1 Requirements

In general, the requirements for numerical simulation of granular material are as follows:

● Particles can be (or must be) of various size and material;

● Resolution up to single particle must be achieved;

11

- Heat and mass transfer between the particles and the fluid must be solved. This means that fluid motion must be simulated at the same time;

- A grid for fluid and particle simulation may be non-uniform and unstructured;

- Therefore, a full description of the particle processes is needed.

IV.1.2 Assumptions

One particle may be in contact with more than one other particle. It is a well known problem of N bodies. Charged particles may influence each other by long-range or short-range forces. On the other hand, particles are no absolutely rigid bodies and, therefore, they deform each other by normal and shear (tangential) forces resulting from elastic collision. Consequently, contact deformation of the particle i with another particle j may influence the contact dynamics of particle i with particle k. Deformation may be plastic and energy dissipation may occur. Contact between particles in granular material may be static and dynamic.

The Hertz theory of contact is applied to the static contact. However, for the dynamic case involving loadings of short duration, estimations of the model parameters are extremely difficult to make due to the vibration of the particles (Sadd *et al.* (1989)). In general, such a problem can not be solved analytically, but has be simulated directly by real body consisting molecules or by the finite element method (Potapov, Hopkins & Campbell (1995), and Potapov, Campbell & Hopkins (1995)). Such an approach can be applied to several particles, for big systems of particles, however, the computational expenditure will be too high.

Therefore the following assumptions are made:

1. The contact between the particles i and j will not influence the dynamics of the contact between the particles i and j. Therefore, the dynamics of each particle is determined by the sum of all collisions forces at the same time, which can be calculated independently.

2. Particle deformations are elastic. This means that the particle shape after a collision is the same as before the collision.

Deformation is simulated by a particle overlap (Figure 3), which means that the particle shapes will not be changed during collision.

IV.2.1 Common Scheme
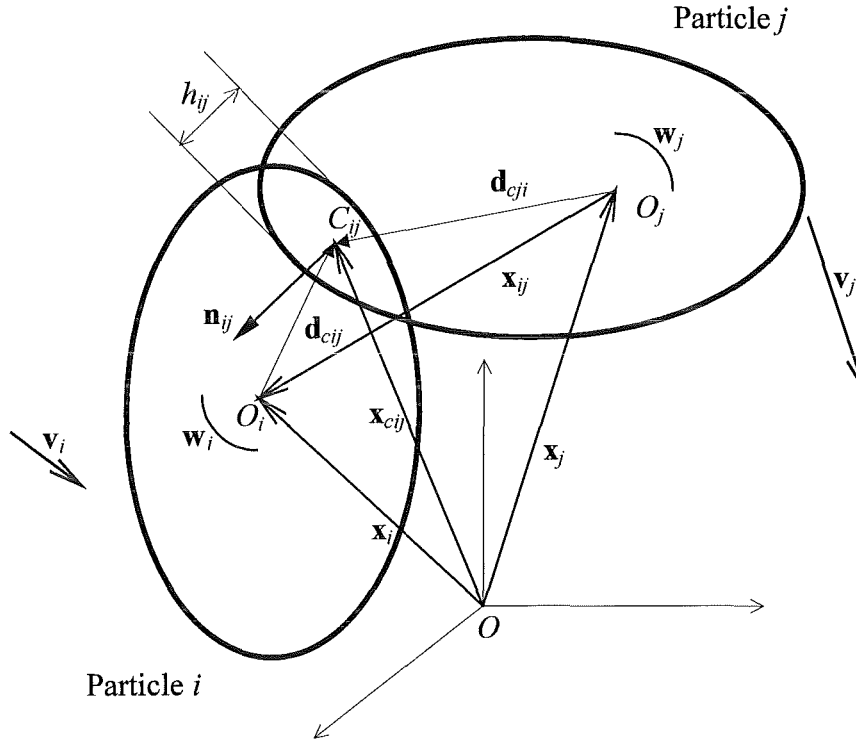
Figure 4. Geometry of overlapping contact of two elastic particles

For a vector $\mathbf{F}$, its modulus may be written as F or as $|\mathbf{F}|$

$$F = |\mathbf{F}| \tag{1}$$

For a decomposition of a vector into a normal and a tangential component, the normal component will be with denoted "n", the tangential component "t". The origin of the non-moving laboratory coordinate system is located in the point O.

Two particles i and j are in collisional contact with the positions $\mathbf{x}_i$ and $\mathbf{x}_j$ of the particles, the centres of gravity O_i and O_j, the velocities $\mathbf{v}_i$ and $\mathbf{v}_j$, and the angular velocities $\mathbf{w}_i$ and $\mathbf{w}_j$. The vector $\mathbf{x}_{ij}$ of the relative position points from the centre of gravity of particle i to that of particle j

$$\mathbf{x}_{ij} = \mathbf{x}_i - \mathbf{x}_j \tag{2}$$

The contact point C_{ij} is defined to be in the centre of the overlap area with the position vector $\mathbf{x}_{cij}$. The depth of overlap is h_{ij}. $\mathbf{n}_{ij}$ is a unit vector into the normal direction of the contact surface through the centre of the overlap area from the contact points to the inside of the particle i (Figure 4)

$$\mathbf{n}_{ij} = -\mathbf{n}_{ji} \qquad\qquad (3)$$

The vectors $\mathbf{d}_{cij}$ and $\mathbf{d}_{cji}$ point from the centre of the particles to the contact point C_{ij} (Figure 4)

$$\mathbf{d}_{cij} = \mathbf{x}_{cij} - \mathbf{x}_i \qquad\qquad (4)$$
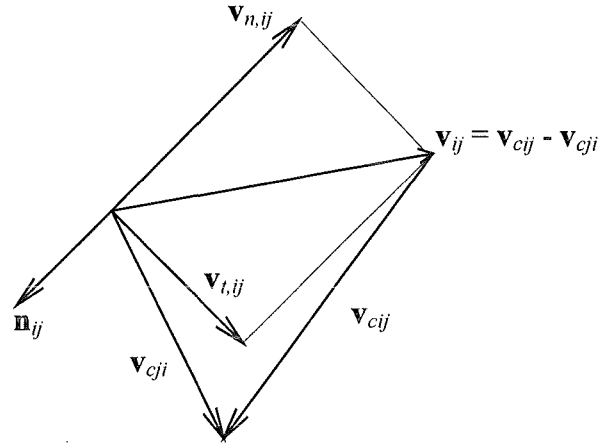
Figure 5. Scheme of relative velocity vectors

The relative velocity of the contact point (Figure 5) is defined as

$$\mathbf{v}_{ij} = \mathbf{v}_{cij} - \mathbf{v}_{cji} \qquad\qquad (5)$$

where

$$\mathbf{v}_{cij} = \mathbf{v}_i + \mathbf{w}_i \times \mathbf{d}_{cij} \qquad\qquad (6)$$

$$\mathbf{v}_{cji} = \mathbf{v}_j + \mathbf{w}_j \times \mathbf{d}_{cji} \qquad\qquad (7)$$

are the velocities of the particles i and j at the contact point. It holds that $\mathbf{v}_{ij} = -\mathbf{v}_{ji}$. The normal component of the relative velocity is defined as

$$\mathbf{v}_{n,ij} = \left(\mathbf{v}_{ij} \cdot \mathbf{n}_{ij}\right)\mathbf{n}_{ij} \qquad\qquad (8)$$

Then, the relative velocity can be expressed as the sum of normal and tangential components. Therefore, the shear (tangential) component of the relative velocity can be calculated by the equation

$$\mathbf{v}_{t,ij} = \mathbf{v}_{ij} - \mathbf{v}_{n,ij} \qquad\qquad (9)$$

The tangential forces act at the contact point. For contact with partial slip particles may slip relatively the distance $\delta_{t,ij}$ in the tangential direction. $\delta_{t,ij}$ is the integrated slip in the tangential direction after the particles i and j came into contact and can be defined by the equation (Haff (1993))

14

$$\delta_{t,ij} = \left| \int \mathbf{v}_{t,ij}(t)dt \right| \qquad (10)$$

$\delta_{t,ij}$ is allowed to increase until the tangential force exceeds the limit imposed by static friction.

Now, the vector of tangential displacement $\delta_{t,ij}$ is defined to be perpendicular to the normal contact direction and located on the same line as $\mathbf{v}_{t,ij}$. The modulus of $\delta_{t,ij}$ is defined by (10). If the tangential component of the contact velocity $\mathbf{v}_{t,ij}$ is not equal to zero, then the unit vector $\mathbf{t}_{ij}$ of the tangential contact direction is directed along $\mathbf{v}_{t,ij}$. If $\mathbf{v}_{t,ij}$ is equal to zero, $\mathbf{t}_{ij}$ has the same direction in which the slip occurs. Otherwise $\mathbf{t}_{ij}$ is equal to zero if $\mathbf{v}_{t,ij}$ and $\delta_{t,ij}$ are equal to zero.

$$\mathbf{t}_{ij} = \begin{cases} \dfrac{\mathbf{v}_{t,ij}}{\left| \mathbf{v}_{t,ij} \right|}, & \mathbf{v}_{t,ij} \neq 0 \\[2ex] \dfrac{\delta_{t,ij}}{\left| \delta_{t,ij} \right|}, & \mathbf{v}_{t,ij} = 0, \ \delta_{t,ij} \neq 0 \\[2ex] 0, & otherwise \end{cases} \qquad (11)$$

IV.2.2 Particle Shapes

Particles can be represented by spheres, ellipsoids, superquadrics, polyhedrons, *etc.* in three dimensions, or by disks, ellipses, polygons, polar forms, *etc.* in two dimensions or by strings in one dimension. Reviews of various possible shapes of particles and some aspects of applications of shapes are presented in Haff (1993) and Ristow (1994b). It is no problem to construct particles in various shapes. The major problem is to detect the overlap and to calculate the intersection points, overlap area, contact point and normal and tangential contact vectors. For some analytical shapes, such as ellipsoids or superquadrics, analytical solutions can be found. For more complicated shapes, however, a considerable computational expenditure is required.

SPHERICAL PARTICLES. The most popular shape of particles is the sphere for three- (*e.g.* Lubachevsky *et al.* (1996), Kornilovsky *et al.* (1996)) and two-dimensional particles (*e.g.* Lubachevsky (1991), Sadd *et al.* (1993), Hoomans *et al.* (1996), Luding *et al.* (1996), Kumaran (1997)) with the center of gravity being located at the geometrical centre. This especially applies to Molecular Dynamics simulations, because it is quite natural to describe an atom as a sphere (*e.g.* Grest *et al.* (1989), Glikman *et al.* (1996)). It is described by the radius only and no orientation is needed. A disc was used to simulate three-dimensional cylinders which are all oriented in the same direction and located on the same plane (Campbell and Brennen (1985)).

For spheres it writes as follows

$$h_{ij} = R_i + R_j - \left| \mathbf{x}_{ij} \right| \tag{12}$$

$$\mathbf{n}_{ij} = \begin{cases} 0, \mathbf{x}_{ij} = 0 \\ \dfrac{\mathbf{x}_{ij}}{\left| \mathbf{x}_{ij} \right|} \end{cases} \tag{13}$$

$$\mathbf{d}_{cij} = -\left(R_i - \tfrac{1}{2} h_{ij} \right) \mathbf{n}_{ij} \tag{14}$$

where R_i the is radius of the spherical particle.

ELLIPSOIDAL PARTICLES. Ellipses for two-dimensional particles and ellipsoids for three-dimensional particles are other often used shapes, because various kinds of granular material particle resemble these shapes. Therefore, the characteristics of granular material are better represented by systems of ellipsoidal particles than by systems of spherical particles (Rothenburg and Bathurst (1991)). For discussions of the implementation of ellipses and ellipsoids see Lin and Ng (1995), Lin and Ng (1997).

Ting and Corkum (1992), Ting *et al.* (1993) and Kohring (1993) used two-dimensional ellipse - shaped particles to simulate granular material by the Discrete Element Method (DEM). Intersection points can be calculated by solving the *quartic equation* which results from the combination of the equations of two ellipses in contact (Ting (1991) and Rothenburg and Bathurst (1991)). The algorithm proposed by Rothenburg and Bathurst (1991) is similar to the algorithm of Ting (1991) and minor differences occur in the formulation of the quartic

equation. However, the method of quartic equation can not be extended easily to a three-dimensional problem (Lin and Ng (1995)).

Ellipse 1

Point 1

Point 2
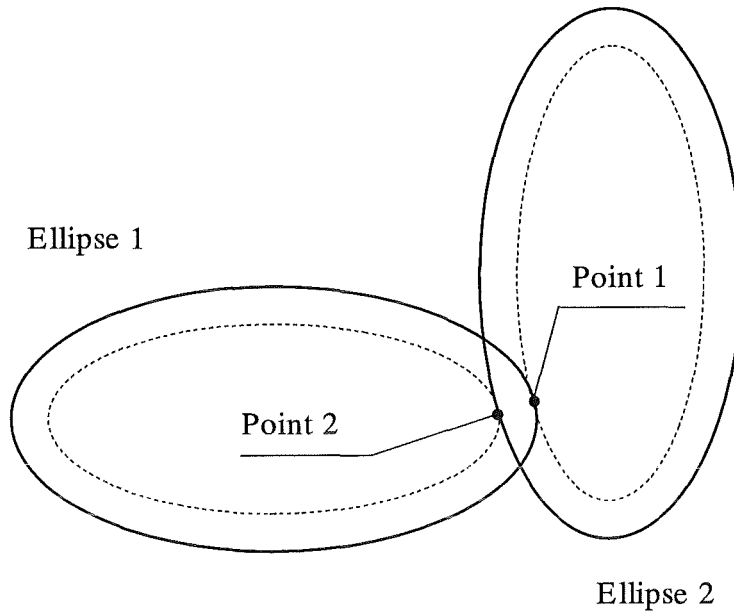
Ellipse 2

Figure 6. Contact detection of ellipsoids based on the geometrical potential concept (according to Lin and Ng (1995))
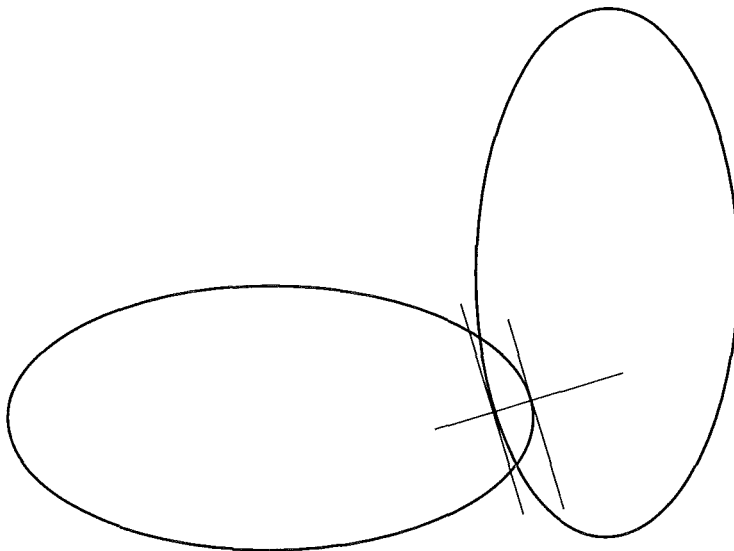
Figure 7. Contact detection of ellipsoids based on the common normal concept (according to Lin and Ng (1995))

Lin and Ng (1995) describe two other contact detection algorithms for ellipses and ellipsoids. One algorithm proposed by Ng is based on the geometrical potential concept. The ellipse is defined by the function of $f(x,y) = 0$. The varying value of the potential $f = f(x,y)$ represents a family of geometrically similar ellipses of various size sharing the same origin. There exists a point (Point 1) on Ellipse 1, which forms the lowest potential (smallest f) of the other ellipse

(Ellipse 2). If the point is inside or on Ellipse 2 (*i.e.* $f(x_1,y_1) \leq 0$), a contact exists. The line connecting these two points 1 and 2 is considered to be the normal of the contact. The same method was applied to three-dimensional ellipsoids. In general, however, the normal vectors of the ellipsoids at point 1 and point 2 are not parallel. For this case, another contact detection algorithm was proposed, which is based on a common normal vector for ellipsoids in the overlapped area (Figure 7). For both algorithms the errors and the CPU time consumption for contact detection were compared and the algorithm based on the geometrical potential was found to be more favourable in terms of accuracy and efficiency and was used for later simulations in Lin and Ng (1997).

Allen *et al.* (1989) used the Vieillard-Baron criterion for the overlap between two ellipsoids. Perram *et al.* (1984), Perram and Wertheim (1985) and Camp and Allen (1996) used prolate and oblate uniaxial three-dimensional ellipsoids of equal volume to simulate the hard convex body by the constant-pressure Monte Carlo method. For overlap detection, they used the Perram-Wertheim overlap criterion (contact function). For more details, see in Perram *et al.* (1984) and Perram and Wertheim (1985).

SPHERO-CYLINDERS. Allen *et al.* (1989) discussed the use of sphero-cylinders for the simulation of Molecular Dynamics.

SUPERQUADRICS and *HYPERQUADRICS.* A wide range of various shapes of particles can be generated economically using generalized ellipsoids, called superquadrics. The general equation of three-dimensional superquadrics is given by (Williams and Pentland (1992)):

$$F(x, y, z) = \sum_{i=1}^{3} \left| \frac{x_i}{a_i} \right|^{\varepsilon_i} - 1 = 0 \tag{15}$$

where $x_1 = x$, $x_2 = y$, $x_3 = z$, a_i determine the length of the principal axes, ε_i is the power, such that $0 < \varepsilon_i < \infty$. According to Williams and Pentland (1992), it is estimated that 80% of shapes of solids can be represented by the superquadrics. Other shapes of solids can be derived from superquadrics in higher dimensions - hyperquadrics (Williams and Pentland (1992)).

POLAR SHAPE. Oakeshott and Edwards (1994) and Hogue and Newland (1994) proposed to represent two-dimensional particles in the polar form (Figure 8). The shape of each particle is represented by vertices that are joined by small line segments. To describe the particle shape, the length and angle from a reference point at 0 radians of the vertices are needed. Hogue and Newland (1994) used an average of 24 vertices for particle simulation. For the polar shape, the detection of particle-particle and particle-wall contacts is rather easy.

18
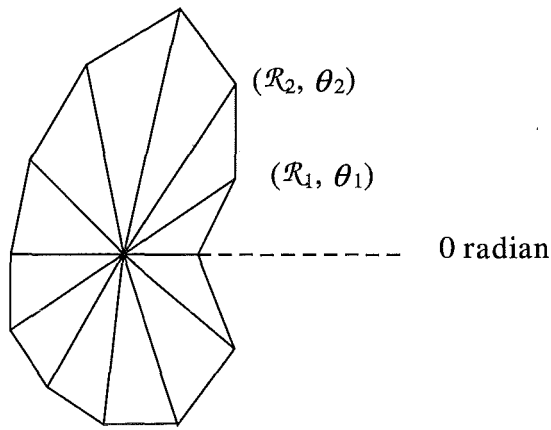
Figure 8. Shape of particle represented in the polar form (according to Hogue and Newland (1994))

Nolan and Kavanagh (1995) mentioned the proposal made by Cheng and Sutton to define the shape and size of particles in terms of polar coordinates and subsequent Fourier series. Due to a mistake in the references list of Nolan and Kavanagh (1995), however, it was impossible to find this references. Nolan and Kavanagh (1995) confirmed that this model can successfully define the location of the closed surface, whereas it is unable to determine whether the surface of one shape overlaps the surface of another.

SHAPE SKELETON METHOD. The idea underlying this method occurred when reading Vimawala and Turkiyya (1997). The particle can be constructed by some lines which may be called "shape skeleton". The shape of such a particle is defined by "rays" containing information on the minimum distances to the shape boundary from various locations along the skeleton. Of course, it is a memory consuming method, but if all rays of the particle to be defined are of the same length, only the additional parameters of the skeleton line need to be kept in the memory.

POLYGON SHAPE. Hopkins (1992) and Kohring (1995b) used particles with the shape of an arbitrary polygon for the two-dimensional simulation of granular material (Figure 9). The extension of this method to three-dimensional particles is not easy and rather memory demanding.
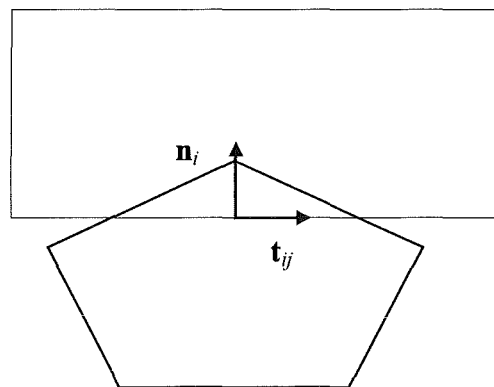
Figure 9. Contact geometry of particles represented by polygons

COMPOSITE PARTICLES. Gallas and Sokolowski (1993) proposed a model to simulate the behaviour of granular material with non-spherical particles that are composed of *glued spheres* (Figure 10). Spheres with the same radius were connected by a stiff bar.
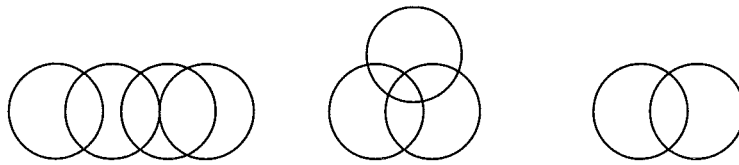
**Figure 10. Non-spherical particles composed of identical spheres
(according to Gallas and Sokolowski (1993))**

A similar algorithm of composing a particle of spheres was proposed by Nolan and Kavanagh (1995). They demonstrated the efficiency of a method using cylindrical, bean- and nail-shaped particles. Overlaps of two adjacent particles can be detected easily by checking each component sphere within one particle with every component sphere in the other particle. In this algorithm, the restoring force of the particles is the vector sum of the restoring forces of the individual component spheres which make up the particle shape.

Poschel and Buchholtz (1993), Buchholtz and Poschel (1994) and Maeno (1996) used a similar approach to simulate two-dimensional particles. In this model, each particle consists of five glued spheres or discs (Figure 11). Four of them are located at the corners of a square of size L. The fifth sphere is situated in the middle of the square and its radius is chosen to touch the others. Each sphere in the particle is connected with neighbours spheres by springs. It is interesting, that this model reproduces static friction effects better than conventional methods (Buchholtz and Poschel (1994)).
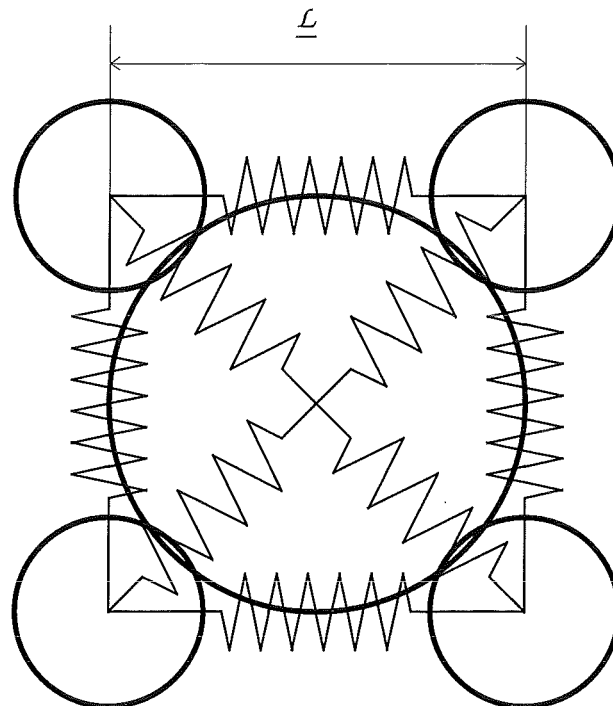
**Figure 11. Shape of a non-spherical particle consisting of five spheres
(according to Poschel and Buchholtz (1993))**

20

Potapov, Hopkins and Campbell (1995) and Potapov, Campbell and Hopkins (1995) constructed a two-dimensional particle using *glued polygons* such as triangles or Voronoi polygons. Due to the high expenditure of the method, it can be used to simulate particle systems consisting of a small number of particle.

VIRTUAL SPACE METHOD. Finally, another possibility to describe a particle of arbitrary shape in space shall be proposed. A space is divided into discrete cells – pixels, named "virtual space". Initially, the virtual space is empty, which means that the value of the pixels is zero. Each particle has a method to describe itself in space by filling the cells in this virtual space, adding 1 to value of pixels. For saving calculation time and memory, particles 1 and 2 fill the virtual space only in the area of possible contact (Figure 12). The pixels have the value of 2 in the common overlap and this area is easy to analyse for possible contact and parameters of contact. It is a straightforward method and, therefore, the simplest, but not the fastest. However, it is very easy to construct other methods with only the common overlap space being filled by 1. Thus, the advantages of fast logical bitwise computer operators could be made use of.
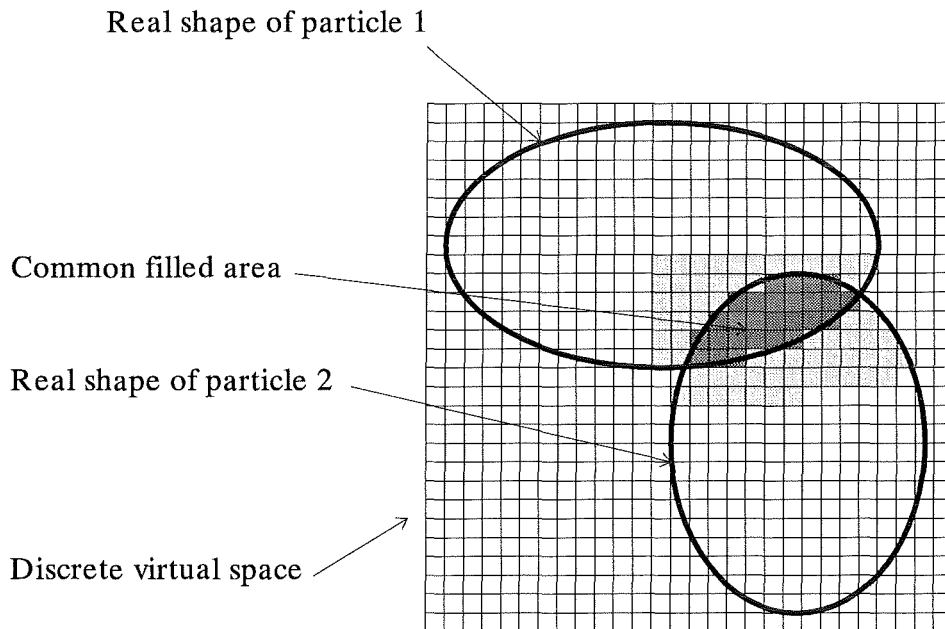
Figure 12. Particle in the virtual space

21

IV.2.3 Problem of Contact Point Definition

The importance of accurate calculations of both the contact point and normal vector was stressed by Hogue and Newland (1994). They pointed out that errors of more than 10 degrees may lead to non-realistic particle motion. Up to now, however, there is no common agreement on how to set the contact point. The various algorithms depend on the particle shapes and the methods to detect the contact.
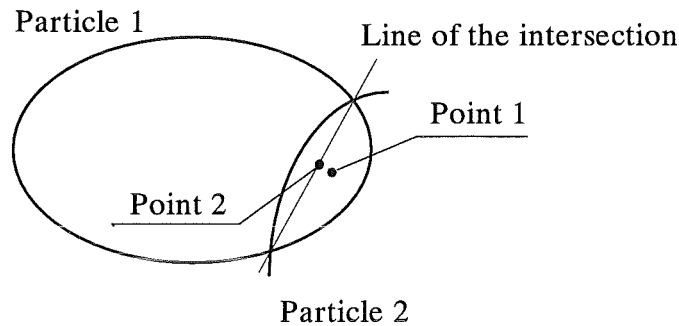
Figure 13. Problem of contact point definition

The first method specifies the contact point to be in the middle of the overlap area as it was pointed out above (point 1 in Figure 13). The method defines the contact point to be in the middle of the line between the intersection points (point 2 in Figure 13). For three dimensional particles this corresponds to a surface of intersection and a contact line. The possible errors of the second method are evident when the particle (*e.g.* sphere) collides with the wall which can be treated as a sphere with an infinite radius. If the contact point is set to be on the line of intersection, then it means that the wall will be not deformed during collision. This is true only for an infinitely rigid wall. We suppose that if the contacting particles are of the same material, then the contact point defined to be in the middle of the contact area more accurate than that point obtained by the line intersection method.

IV.2.4 Boundary Conditions

The properties of granular flow are strongly dependent on the boundary conditions at the wall (Thompson and Grest (1991)). Therefore, the setting up of boundary conditions is very important for a correct simulation of the granular material behaviour.

Several types of boundary conditions can be used:

- free inflow or outflow

- periodic

- walls that may be moving or stationary

FREE INFLOW and *FREE OUTFLOW BOUNDARIES* imply free inlet and outlet conditions for the particles through the boundaries of the calculation space, outside of which the particles are not included into the calculations.

PERIODIC BOUNDARY CONDITIONS (PBCs) mean that particles exiting at one edge of the simulation space enter at the opposite edge with the same dynamic parameters - velocity, rotation *etc.* (Figure 14). In Figure 14, particle 1 is on the edge, to which the periodic boundary condition is applied. Particles 1' and 4' do not exist in the calculations, but are copies of particles 1 and 4, which are used for the contact calculations of particle 4, which is crossing the periodic boundary. Grest *et al.* (1989) proposed to use "ghost" particles that are near the boundaries (for example particles 1 and 4), have copies in the surrounding space (for example, particles 1' and 4') and are created or deleted for the calculations, if necessary.

Calculation region
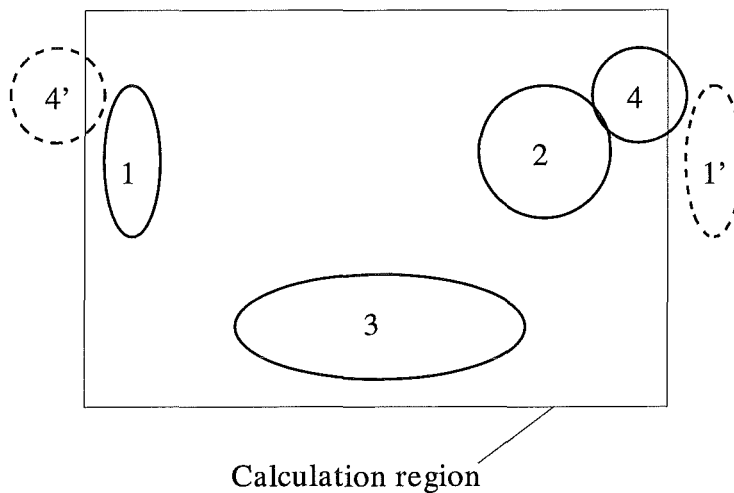
Figure 14. Periodic boundary conditions

If periodic boundary conditions are applied in x direction with the period L_x, then any function f, which may be a vector function, can be written as

$$f(x + L_x) = f(x) \qquad (16)$$

Periodic boundaries are very useful to simulate a relatively small number of particles and, therefore, widely used to simulate particle motion (*e.g.* Rapaport (1980), Campbell and Brennen (1985), Lubachevsky (1991), Camp and Allen (1996), Ristow *et al.* (1997)). Van Gunsteren *et al.* (1984) used periodic truncated octahedronal boundary conditions. See Grest *et al.* (1989), Allen and Tildesley (1990) and Shrinivasan *et al.* (1997) for discussions concerning the implementation of periodic boundary conditions with improved software code vectorization.

However, difficulties may arise from the use of periodic boundary conditions:

- It is impossible, at least in the most straightforward applications of PBCs, to study accelerating flows (Haff (1993)).

- Care must be taken when simulating processes which may be periodic in space with the period L_p, because this period will be influenced by period of PBCs L as

$$L_p = \frac{L}{n}, \, n = 1, 2, 3, \ldots \tag{17}$$

WALLS can be constructed by planes, spheres, cylinders or other shapes as big particle, or by array of small particles (Figure 15). Of course, walls can move and rotate around a point of rotation.
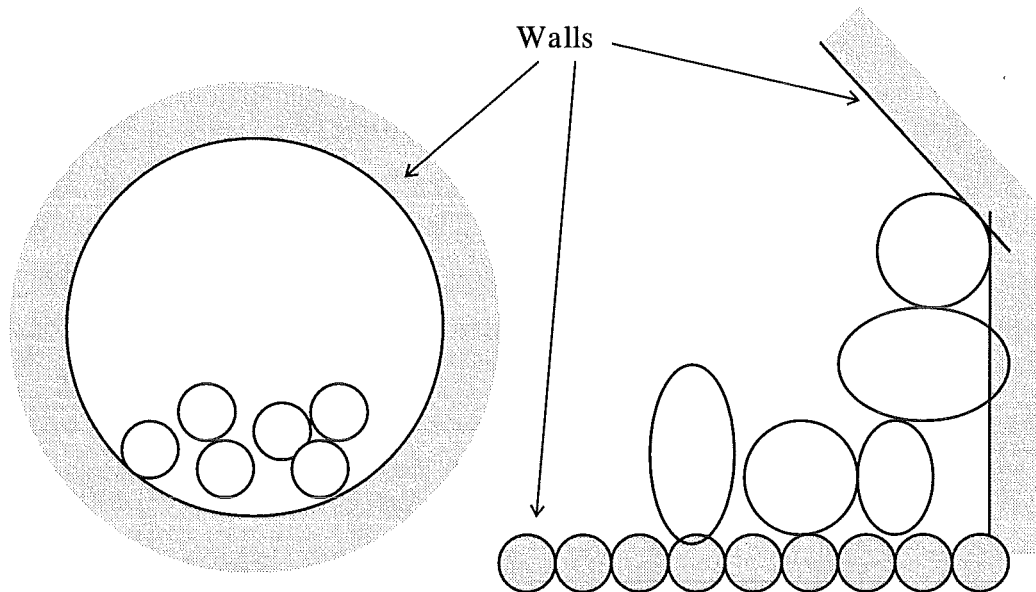
Figure 15. Constructions of walls

Walls constructed by planes may be treated as particles with an infinite radius and mass. A rotary kiln can be constructed by a cylinder or sphere with a negative radius. Collisions between particles and walls are defined by the material and geometry of the particles and walls as in the case of collisions between particles. Campbell and Brennen (1985) proposed other types of walls. Type A applies when the wall surface is rough in the sense of zero relative tangential slip existing between the particle surface and the wall after the collision. The type B wall is characterised with non-slip conditions, which means that after the particle-

wall collision the particle centre assumes the same tangential velocity with no change in its rotation rate.

It is convenient to construct rough walls by an array of particles (*e.g.* Thompson and Grest (1991)) especially for molecular dynamics simulations (*e.g.* Din and Michaelides (1997)). But this method may involve a high expenditure especially for the three-dimensional case.

Possible problems:

- Geometrical problem of contact detection may arise on the junctions of the walls (corners), especially if the walls are constructed by planes.

- If particles are in the fluid, then the wall influence on the fluid motion and the influence of sheared fluid flow on the motion of particles may be worth to be considered, especially for non-spherical particles (Gavze and Shapiro (1997)).

IV.3 EQUATIONS OF PARTICLE MOTION

The behaviour of granular media can be simulated by direct calculations of classical Newtonian dynamics equations of the second Newton law for each particle in the material.

Equations of particle motion include a system of equations for the translational motion of the centre of gravity and for the rotational motion around the centre of gravity.

IV.3.1 Translational Motion

Translational motion of the centre of gravity of a particle i can be fully described by a system of equations (Landau and Lifshitz (1960)):

$$m_i \frac{d^2 \mathbf{x}_i}{dt_2} = m_i \mathbf{a}_i = \mathbf{F}_i \tag{18}$$

$$\mathbf{v}_i = \frac{d\mathbf{x}_i}{dt} \tag{19}$$

where $\mathbf{v}_i$, $\mathbf{a}_i$ and $\mathbf{x}_i$ are vectors of velocity, acceleration and the position of the centre of gravity m_i of the particle i ($i = [1, N]$), N is the number of particles in the granular material. $\mathbf{F}_i$ is the sum of all forces acting on the centre of gravity of the particle

$$\mathbf{F}_i = \mathbf{F}_{i,contact} + \mathbf{F}_{i,gravity} + \mathbf{F}_{i,fluid} + \mathbf{F}_{i,buoyancy} + \mathbf{F}_{i,external} \tag{20}$$

where $\mathbf{F}_{i,contact}$ is the summation of the direct contact forces between the particle i and another particle

$$\mathbf{F}_{i,contact} = \sum_{j=1, j \neq i}^{N} \mathbf{F}_{ij} \tag{21}$$

where $\mathbf{F}_{ij}$ is a force acting on the contact area of elastic impacts between the particles i and j. It is evident that

$$\mathbf{F}_{ij} = -\mathbf{F}_{ji} \tag{22}$$

In general, contacting forces can include inter-particle forces acting between charged particles. $\mathbf{F}_{i,gravity}$ is the gravity force acting on the particle

$$\mathbf{F}_{i,gravity} = m_i \mathbf{g} = V_i \rho_i \mathbf{g} \tag{23}$$

ρ_i is the density of the particle i, V_i is the volume of the particle and $\mathbf{g}$ is the gravity acceleration vector, respectively. $\mathbf{F}_{i,buoyancy}$ is the Archimedes buoyancy force on the particle in the surrounding fluid

$$\mathbf{F}_{i,buoyancy} = -V_i \rho_{fluid} \mathbf{g} \tag{24}$$

ρ_{fluid} is the density of surrounding fluid. For the computer code optimisation, the sum of $\mathbf{F}_{i,gravity}$ and $\mathbf{F}_{i,buoyancy}$ may be written as

$$\mathbf{F}_{i,gravity} + \mathbf{F}_{i,buoyancy} = V_i \left(\rho_i - \rho_{fluid} \right) \mathbf{g} \qquad (25)$$

$\mathbf{F}_{i,fluid}$ denotes the fluid drag and fluid lift forces (Langston *et al.* (1996)) acting on the particle *i*. $\mathbf{F}_{i,external}$ is the total of other external forces. For example, if a particle is charged, $\mathbf{F}_{i,external}$ could include the force of the external electromagnetic field.

It is supposed that $\mathbf{F}_{i,external}$, $\mathbf{F}_{i,fluid}$ and $\mathbf{F}_{i,buoyancy}$ are acting on the centre of gravity of the particle. $\mathbf{F}_{i,fluid}$ and $\mathbf{F}_{i,external}$ are not discussed in the present report. More details on inter-particle contact forces $\mathbf{F}_{ij}$ are given below in the chapter "Inter-particle Contact Forces " on the page 29.

The change of mass of particles due to combustion or abrasive wear may be included in the equations of particle motion. The combustion model, developed by Peters (1997), consists of a set of non-linear differential equations, of which the solution describes the mass loss of particles due to chemical reaction in a packed bed. Yevtushenko and Kulchytsky-Zhyhailo (1997) consider rigid and elastic half-spaces with a sliding contact in an elliptical region, where abrasive wear reduces the mass of particles. The abrasive wear was described by Archard's law, for which the rate of material removal is proportional to the pressure and the speed in the contact region.

IV.3.2 Rotational Motion

Rotational motion of the particle i around the centre of gravity can be fully described by the following system of equations (Landau and Lifshitz (1960)):

$$I_i \frac{d^2\theta_i}{dt^2} = I_i \mathbf{u}_i = \mathbf{T}_i \tag{26}$$

$$\mathbf{w}_i = \frac{d\theta_i}{dt} \tag{27}$$

where θ_i, $\mathbf{w}_i$ and $\mathbf{u}_i$ are the vectors of orientation, angular velocity and angular acceleration of the particle i, I_i is the inertial tensor of the particle (and always can be made diagonal $I_i = (I_{1i}, I_{2i}, I_{3i})$), $\mathbf{T}_i$ is the sum of all torques acting on the particle i

$$\mathbf{T}_i = \mathbf{T}_{i,contact} + \mathbf{T}_{i,fluid} + \mathbf{T}_{i,external} \tag{28}$$

where $\mathbf{T}_{i,contact}$ is the summation of torques caused by the contact forces between the particles

$$\mathbf{T}_{i,contact} = \sum_{j=1,j\neq i}^{N} \mathbf{T}_{ij} = \sum_{j=1,j\neq i}^{N} \mathbf{d}_{cij} \times \mathbf{F}_{ij} \tag{29}$$

where $\mathbf{d}_{cij}$ is the vector of relative contact positions according to Figure 4. $\mathbf{T}_{i,fluid}$ is the summation of the torque caused by anti-symmetrical fluid drag forces, $\mathbf{T}_{i,external}$ denotes the summation of torques caused by other external forces.

Some authors did not consider rotation in the simulation of particle motion to be important (*e.g.* Tagucki (1992b), Kalthoff *et al.* (1996), Lee and Herrmann (1993)). But rotation of the particles could be important for repulsion between particles in contact and dissipation of energy during collision (Lee and Herrmann (1993)).

IV.3.3 Inter-particle Contact Forces
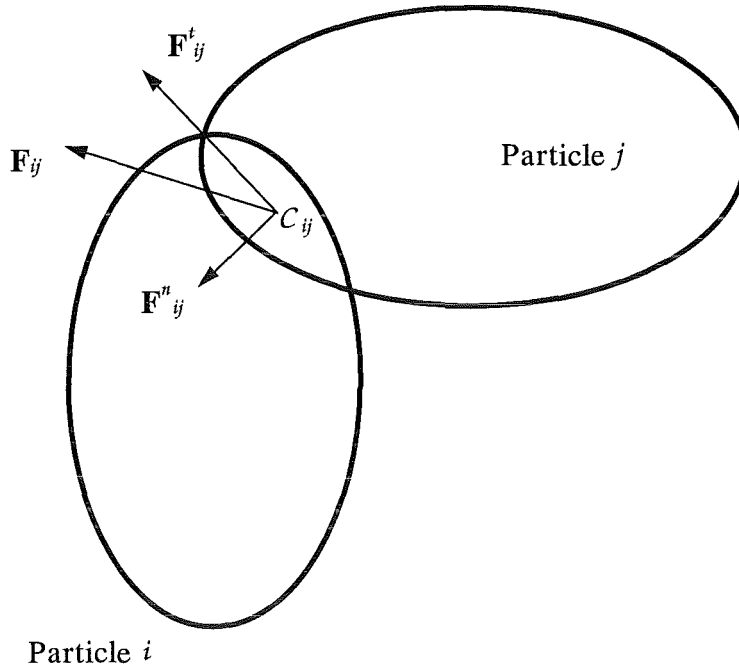
Figure 16. Forces acting on the contact point of particle i with particle j

According to Kohring (1995), a model of inter-particle visco-elastic contact forces has to describe the following four effects:

1. particle elasticity;

2. energy loss through internal friction;

3. attraction on the contact surface;

4. energy loss due to surface friction.

The contact force $\mathbf{F}_{ij}$ of a visco-elastic collision between the two particle i and j acts on the contact point and can be expressed as the sum of normal and tangential components

$$\mathbf{F}_{ij} = \mathbf{F}_{n,ij} + \mathbf{F}_{t,ij} \tag{30}$$

which, in the general form, would be functions of the relative normal $\delta_{n,ij}$ and tangential $\delta_{t,ij}$ displacements of contact as well as of the relative normal and tangential velocities (Sadd *et al.* (1993))

$$\mathbf{F}_{n,ij} = \mathbf{F}_{n,ij}\left(\delta_{n,ij}, \mathbf{v}_{n,ij}, \delta_{t,ij}, \mathbf{v}_{t,ij}\right) \tag{31}$$

$$\mathbf{F}_{t,ij} = \mathbf{F}_{t,ij}\left(\delta_{n,ij}, \mathbf{v}_{n,ij}, \delta_{t,ij}, \mathbf{v}_{t,ij}\right) \tag{32}$$

IV.3.3.1 Normal Component of Contact Force

The most general form of the contact forces is given by Kohring (1996). According to him, the normal components of the contact forces can be expressed as the sum of the elastic repulsion forces, internal friction and the surface attraction force of a particle.

$$\mathbf{F}_{n,ij} = \mathbf{F}_{n,ij,elastic} + \mathbf{F}_{n,ij,viscous} + \mathbf{F}_{n,ij,surface} \qquad (33)$$

IV.3.3.1.1 Elastic Repulsion Force

In literature, many models for elastic repulsion forces can be found. Mostly, the models were used for spherical particles in three-dimensional simulations and for disks in two-dimensional simulations. In these cases, the models can be simplified. But in general, a model for the normal repulsion force depends on the contact geometry and on the properties of the particle material. In some cases, ellipsoid particles or particles represented by polygons or in the polar form were simulated. Almost all models simulated particles with the same material properties. It is possible to divide these models into several main groups according to the dependency of the repulsion force on the overlap depth:

- linear models

- non-linear models

- models with hysteresis

- continuous interaction (or short-range force) models.

LINEAR MODELS: One of the most popular models of elastic repulsion force, which was widely used for spherical particles or cylinders, is based on the linear Hooke's law of a spring with a spring stiffness constant $K_{n,ij}$ (Ristow *et al.* (1997), Thompson and Grest (1991), Quwerkerk (1991), Tsuji *et al.* (1993), Taguchi (1992b), Haff and Werner (1986), Ting and Corkum (1992), Ting *et al.* (1993))

$$\mathbf{F}_{n,ij,elastic} = K_{n,ij} h_{ij} \mathbf{n}_{ij} \qquad (34)$$

which applies when it can be assumed that there is no deformation out of contact area and plane strain conditions exist (Sadd *et al.* (1993)). The major problem is the right selection of the spring stiffness constant $K_{n,ij}$ which, in general, depends on the properties of the material and the contact geometry (Landau and Lifshitz (1959)). Some authors (*e.g.* Gallas and Sokolowski (1993), Gallas *et al.* (1992), Ristow (1992b), Poschel and Buchholtz (1993), Buchholtz and Poschel (1994)) used K equalling Young's elastic modulus E for spherical particles with the same material. To account for the influence of the particle radius on the spring stiffness, Dury and Ristow (1997) used the following expression of $K_{n,ij}$

$$K_{n,ij} = k_{n,ij} R_{ij} \qquad (35)$$

where $k_{n,ij}$ is the material stiffness constant and R_{ij} is the equivalent radius. For spherical particles in contact with the radii R_i and R_j, it is expressed as

$$R_{ij} = \frac{R_i R_j}{R_i + R_j} \qquad (36)$$

If the size of the spherical particles does not vary in a large range and all particles have the same elastic properties, the dependence of $K_{n,ij}$ on the particle radii is weak and can be neglected. Then, $K_{n,ij}$ can be calculated for the average radius (Ristow (1994b), Ristow and Dury in private communication (1997)).

Due to the differences between the predictions of static contact theory and the real contact dynamics, Sadd *et al.* (1993) introduced an experimental stiffness ratio α and the spring stiffness constant. Equation (34) was changed by inserting the dynamic stiffness constant $K_{n,ij,dynamic}$, *i.e.*

$$\mathbf{F}_{n,ij,elastic} = K_{n,ij,dynamic} h_{ij} \mathbf{n}_{ij} \qquad (37)$$

and

$$K_{n,ij,dynamic} = \alpha \, K_{n,ij,static} \qquad (38)$$

where the static stiffness constant $K_{n,ij,static}$ is derived from Hertz theory. For the case of two cylinders with thickness h, $K_{n,ij,static}$ may be expressed as

$$K_{n,ij,static} = \frac{\pi \, h E_i E_j}{2\left(E_i + E_j\right)} \qquad (39)$$

NON-LINEAR MODELS: Another popular model is based on the theory of Hertz, according to which the repulsion force of the deformed particles depends on the compression length h_{ij} (see Figure 3) by the power of 3/2. This model was used for spherical particles or cylinders (Kohring (1996), Ristow (1992b), Buchholtz and Poschel (1993), Lee and Herrmann (1993), Form *et al.* (1993), Ristow and Herrmann (1994c), Ristow (1992b)) and for elliptical particles (Lin and Ng (1997)). According to the Hertz theory, the normal repulsion force for general curved surfaces can be expressed as (Landau and Lifshitz (1959))

$$\mathbf{F}_{n,ij,elastic} = \frac{4}{3} \cdot \frac{E_i E_j}{E_i\left(1 - \sigma_j^2\right) + E_j\left(1 - \sigma_i^2\right)} \sqrt{R_{ij}} \, h_{ij}^{\frac{3}{2}} \mathbf{n}_{ij} \qquad (40)$$

E_i is elastic Young's modulus, σ_i is the Poisson ratio and R_{ij} is the equivalent radius

$$R_{ij} = \frac{1}{2\sqrt{AB}} \qquad (41)$$

where the quantities A and B are related to the radii of curvature R and R' of the particles i and j at the contact point and can be calculated from the followings system of equations (Landau and Lifshitz (1959))

$$2(A + B) = \frac{1}{R_i} + \frac{1}{R'_j} + \frac{1}{R_j} + \frac{1}{R'_j} \qquad (42)$$

31

$$4(A - B) = \left(\frac{1}{R_i} - \frac{1}{R_j} \right)^2 + \left(\frac{1}{R_i'} - \frac{1}{R_j'} \right)^2 + 2\cos 2\phi \left(\frac{1}{R_i} - \frac{1}{R_j} \right)\left(\frac{1}{R_i'} - \frac{1}{R_j'} \right) \tag{43}$$

where ϕ is the angle between the normal sections, whose radii of curvature are R_i and R'_i. For spherical particles $R'_i = R_i$ and $A = B$ - therefore R_{ij} can be calculated by equation (36).

According to Ristow (1994b), Kohring (1994) and Cantelaube *et al.* (1995), the general equation could be written, combining Hooke's law and Hertz theory

$$\mathbf{F}_{n,ij,elastic} = \frac{4}{3} \cdot \frac{E_i E_j}{E_i\left(1 - \sigma_j^2\right) + E_j\left(1 - \sigma_i^2\right)} R_{ij}^{2-\alpha} h_{ij}^{\alpha} \mathbf{n}_{ij} \tag{44}$$

where for the Hertz contact model we have $\alpha = 3/2$ and $\alpha = 1$ for Hooke's law.

Sadd *et al.* (1993) used the simplified form of equation (44)

$$\mathbf{F}_{n,ij,elastic} = K_{n,ij} h_{ij}^{\alpha} \mathbf{n}_{ij} \tag{45}$$

with the constant $K_{n,ij}$.

The normal elastic force expressed by equation (44) (and (40)) is expensive to calculate for numerical simulations and difficult to apply to arbitrary shapes, especially for polygons. Therefore, Hopkins (1992) proposed a model for the simulation of contacts between two-dimensional particles, which was used for polygon shapes, where the magnitude of the normal repulsion force is proportional to the overlap area A_{ij} and the stiffness constant $k'_{n,ij}$:

$$\mathbf{F}_{n,ij,elastic} = k'_{n,ij} A_{ij} \mathbf{n}_{ij} \tag{46}$$

This model was also used by Potapov, Hopkins and Campbell (1995) and Kohring *et al.* (1995).

A similar law for three-dimensional contacting particles with an overlap volume V_{ij}

$$\mathbf{F}_{n,ij,elastic} = k'_{n,ij} V_{ij} \mathbf{n}_{ij} \tag{47}$$

could be constructed, but it remains to be checked for how it corresponds to real physics.

Chang *et al.* (1989) modified the theory of Hertz for two-dimensional contacting cylinders and proposed the relationship between normal spring stiffness and normal force

$$K_{n,ij} = \frac{2\pi\, G'}{1 - \sigma} \cdot \frac{1}{2\ln\left(4R_{ij}/a\right) - 1} \tag{48}$$

where

$$a = \sqrt{\frac{4 R_{ij}\left(1-\sigma\right) F_{n,ij}}{\pi \, G'}}$$

with G' denoting an equivalent shear modulus, which is less than the elastic shear modulus when local yielding occurs, R_{ij} is the reduced radius defined by equation (36).

MODELS with HYSTERESIS: Walton and Braun (1986) proposed a partially latching-spring model with a hysteresis (Figure 17) to approximate experimental data.

$$\mathbf{F}_{n,ij,elastic} = \begin{cases} K_1 \, h_{ij} & \text{for loading} \\ K_2\left(h_{ij} - h_{ij,0}\right) & \text{for unloading} \end{cases}$$

(50)

where h_{ij} is the overlap depth after initial contact and $h_{ij,max}$ is the value of h_{ij} with the unloading curve approaching zero. The constants K_1 and K_2 can be calculated from the equation of the restitution coefficient

$$e = \sqrt{\frac{K_1}{K_2}}$$

(51)

and the equation of hysteresis

$$K_2 = K_1 + S\left|\mathbf{F}_{n,ij,elastic}\right|$$

(52)

with the constant S. This model was used by Lan and Rosato (1997) and Khakhar *et al.* (1997).
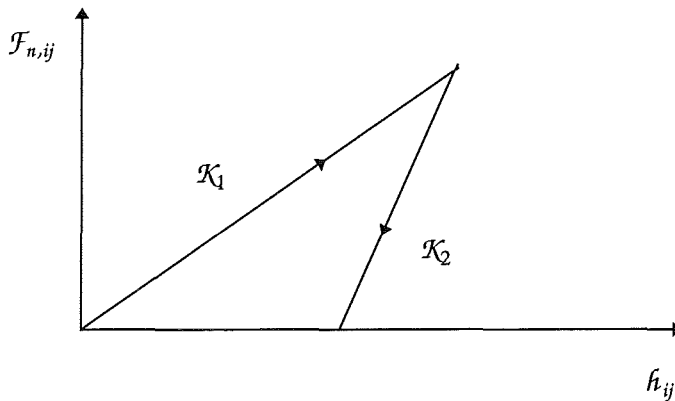
Figure 17. Hysteresis of the normal force - displacement linear law (according to Walton and Braun (1986))

Sadd *et al.* (1993) introduced a more general and sophisticated hysteresis law (Figure 18)

$$F_{n,ij,elastic} = \begin{cases} F_{n,ij,L} = K_{n,ij,L} h_{ij}^p & \text{for loading} \\ F_{n,ij,U} = K_{n,ij,U} h_{ij}^{p+q} & \text{for unloading, re} - \text{unloading} \\ F_{n,ij,rL} = \beta \, F_{n,ij,L} + \left(1 - \beta\right) F_{n,ij,U} & \text{for reloading} \end{cases}$$

(53)

where the values q and β are determined by the overlap depth of loading (unloading and re-unloading) h_{ij}, and p, $K_{n,ij,L}$ and $K_{n,ij,U}$ are defined by material and contact properties.
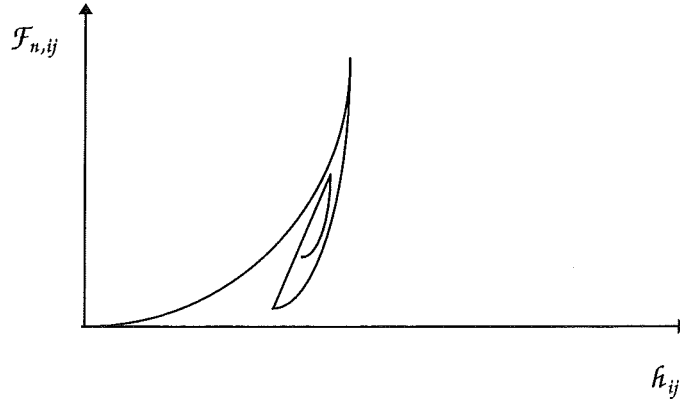
Figure 18. Hysteresis of the normal non-linear force - displacement law (according to Sadd et al. (1993))

The model of Sadd et al. (1993) is non-linear in general and covers the model of Walton and Braun (1986), which is linear. As is obviuos, the model with hysteresis, actually, describes the development of repulsion force and also energy dissipation.

CONTINUOUS INTERACTION MODELS. This model is used in the simulation of molecular dynamics (Verlet (1967), Raparot (1988), Raparot (1991), Raparot (1991b), Raparot (1993), Plimpton (1995), Satoh (1995), Penna et al. (1997), Shrinivasan et al. (1997), Shrinivasan et al. (1997b)) and reused for simulation of granular material (Ristow (1992), Aoki and Akiyama (1995), Akiyama et al. (1996), Langston et al. (1994), Langston et al. (1995)), Langston et al. (1995b)). The method is based on the mechanical models where the force interacts between the centres of particles and on the postulation that the basic features of granular materials can be described by the exclude volume effect and the dissipation of kinetic energy between the granules. The exclude volume is expressed by a short-range repulsive force that interacts between the particles (Akiyama et al. (1996)):

$$\mathbf{F}_{n,ij} = -\frac{\partial V}{\partial \mathbf{x}_{ij}}$$

(54)

where the potential function V may assume the form of the 12-6 Lennard-Jones potential

$$V = \begin{cases} \varepsilon\left[\left(\dfrac{d}{x_{ij}}\right)^{12} - \left(\dfrac{d}{x_{ij}}\right)^{6} + \dfrac{1}{4}\right] & if\ x_{ij} < r_c \\ 0 & otherwise \end{cases}$$

(55)

where

$$r_c = 2^{1/6} d$$

(56)

with d being the characteristic length representing the particle size and ε characteristic energy.

Langston et al. (1994) used a slightly different model where

$$
V = \begin{cases} \varepsilon \left(\dfrac{d}{x_{ij}} \right)^{a} & \text{if } x_{ij} < r_c \\ 0 & \text{otherwise} \end{cases}
\tag{57}
$$

denotes the gravitational force at a separate distance d

$$
\varepsilon = \frac{dmg}{a}
\tag{58}
$$

$a = 36$ and $r_c = 1.8d$ were used for simulations in Langston et al. (1994), $a = 36$ and $r_c = 1.2d$ in Langston et al. (1995b) and $a = 36$ and 144 and $r_c = 1.2d$ for Langston et al. (1995).

IV.3.3.1.2 Surface Attraction Force - Cohesion

The Hertz contact theory is not sufficient to describe contact repulsive forces between bodies. Experiments showed a considerably larger contact area at low loads and tended towards a constant finite value at zero load, while the experimental results nearly corresponded to the predicted values at high loads (Johnson et al. (1971) and Greenwood and Johnson (1981)). This phenomenon was explained by attractive surface forces which became significant as the load was reduced. The importance of surface attraction forces was shown by Kohring (1994).

The surface attraction force is significant for small particles, when atomic and molecular forces are important and can be modelled by an equation which has been derived for spherical particles by Johnson, Kendall and Roberts (1971) (the JKR model), assuming that the surface attraction force only results in a in change of surface energy over the contact area. The model was analysed and adopted by Kohring (1994) and Kohring (1996) as

$$
\mathbf{F}^{n}_{ij,surface} = -\sqrt{\frac{4}{3} \frac{8\pi \, W_{ij} E_i E_j \sqrt{R_{ij}}}{E_i \left(1 - \sigma_j^2\right) + E_j \left(1 - \sigma_i^2\right)}} \, h_{ij}^{3/4} \, \mathbf{n}_{ij}
\tag{59}
$$

where W_{ij} is the surface energy.

Kohring (1994) carried out a numerical simulation of the influence of the surface attraction force on the behaviour of granular material and concluded that for a typical *surface energy* $(W \sim 0.1 \text{ Ws/m}^2)$ the surface attraction force is significant only for particles with a size smaller than 1 mm and can be neglected for particles with a size larger than about 1 cm.

Derjaguin, Muller and Toporov (1975) considered a DMT-model where surface attraction forces have a finite range and, therefore, are acting only just outside the contact zone where the surface separation is small (Thornton and Yin (1991)).

For more discussions concerning the DMT- and JKR-models and the importance of effects of adhesion (surface attraction) for the results of the simulation of granular material behaviour see Tabor (1978), Thornton and Yin (1991), Kohring (1994) and Kohring (1996).

IV.3.3.1.3 Energy Dissipation in the Normal Direction of Contact

Energy dissipates during real collisions between particles. The dissipation can be modelled by the non-conservative viscous force acting during collision. As in the case of repulsive forces various models can be applied.

A very simple and popular model (Haff and Werner (1986), Sadd *et al.* (1989), Gallas *et al.* (1992), Gallas and Sokolowski (1993), Thompson and Grest (1991), Akyiama *et al.* (1996), Ristow and Herrmann (1994c), Dury and Ristow (1997), Poschel and Buchholtz (1993), Buchholtz and Poschel (1993), Buchholtz and Poschel (1994), Maeno (1996), Tsuji *et al.* (1993), Taguchi (1992b), Lee and Herrmann (1993)) is based on the linear dependency of the force on the relative velocity of the particles at the contact point with a constant normal dissipation coefficient γ_n

$$\mathbf{F}_{n,ij,viscous} = -\gamma_n m_{ij} \mathbf{v}_{n,ij} \tag{60}$$

where m_{ij} is the reduced mass of the contacting particles i and j

$$m_{ij} = \frac{m_i m_j}{m_i + m_j} \tag{61}$$

Kohring (1995) and Kohring (1996) used another energy dissipation force model which was derived by Kuwabara and Kono (1987) on the basis of the Hertz elastic theory

$$\mathbf{F}_{n,ij,viscous} = -2 \frac{E_i' E_j'}{E_i'\left(1 - \sigma_j'^2\right) + E_j'\left(1 - \sigma_i'^2\right)} \sqrt{R_{ij} h_{ij}} \, \mathbf{v}_{n,ij} \tag{62}$$

where

$$E_i' = \frac{9\xi_i \eta_i}{3\xi_i + \eta_i} \tag{63}$$

and

$$\sigma_i' = \frac{3\xi_i - 3\eta_i}{2\left(3\xi_i + \eta_i\right)} \tag{64}$$

ξ_i and η_i are the coefficients of viscosity associated with the deformation of the volume and the shear and can be obtained from the attenuation constants of the longitudinal and transverse acoustic waves. These values, however, are difficult to determine. Due to this and the complexity, this model is hardly applied.

Hopkins (1992) proposed a model of energy dissipation on normal direction of contacts between two-dimensional particles (it was used for polygon shapes), where the magnitude of the normal dissipation force is proportional to the rate of change overlap area A_{ij} and the constant normal dissipation coefficient γ_n:

$$\mathbf{F}_{n,ij,viscous} = \gamma'_n \frac{dA_{ij}}{dt} \mathbf{n}_{ij} \qquad\qquad (65)$$

A similar law for three-dimensional contacting particles with an overlap volume V_{ij}

$$\mathbf{F}_{n,ij,viscous} = \gamma'_n \frac{dV_{ij}}{dt} \mathbf{n}_{ij} \qquad\qquad (66)$$

could be constructed, but it remains to be verified how it corresponds to the physical behaviour.

When analysing the normal contact law, Taguchi (1992) proposed a non-linear dependence of energy dissipation on the relative velocity. Further details shall be presented.

As above-mentioned, the model of the normal elastic repulsion force with hysteresis already describes energy dissipation and, therefore, no additional model of energy dissipation is needed.

IV.3.3.1.4 Discussion of Normal Forces

The time of collision between two particles can be deduced from normal forces and calculated analytically for the most simple models.

Assuming two colliding particles with their reduced mass m_{ij}, reduced radius R_{ij} and initial relative velocity $v_0 = v_{ij}(t=t_0)$ at the time t_0, when the collision starts. For an analysis of particle motion under normal forces without surface attraction according to Luding *et al.* (1994) and Taguchi (1992), we can write the second Newton law in the general form for one of the colliding particle

$$m\frac{d^2x}{dt^2} + kx^\alpha + 2\eta m x^\beta \left(\frac{dx}{dt}\right)^\lambda = 0 \qquad (67)$$

where x, d and m are the particle position, size and mass, respectively. Both k and η depend on the particle shape and material as well as on the reduced mass m_{ij}. k depends on Young's modulus and the Poisson ratio, η depends on the shearing and compression viscosities.

For $\alpha = 1$, the second term of the equation expresses the linear Hooke's law for normal repulsion force (equation (34)), for $\alpha = 3/2$ it reflects the Hertz law for normal repulsion force (equation (40)).

For $\beta = 0$ and $\lambda = 1$, the third term of the equation expresses the linear energy dissipation model (equation (60)), for $\beta = \frac{1}{2}$ and $\lambda = 1$, the non-linear energy dissipation model (equation (62)) depending on the overlap depth h_{ij} is chosen.

LINEAR MODELS: For Hooke's contact law ($\alpha = 1$), without energy dissipation ($\eta = 0$) and with the initial relative velocity of the collision v_0 and

$$\omega^2 = \frac{k}{m} \qquad (68)$$

the law of particle motion will be

$$x = \frac{v_0}{\omega}\sin \omega t \qquad (69)$$

$$v = v_0 \sin \omega t \qquad (70)$$

for the time $t < T_c$, where T_c being the time of collision between two particles,

$$T_c = \frac{\pi}{\omega} = \pi\sqrt{\frac{m}{k}} \qquad (71)$$

The value of maximum overlap is expressed as

$$h_{max} = \frac{v_0}{\omega} = v_0\sqrt{\frac{m}{k}} \qquad (72)$$

Of course, the coefficient of restitution, e, equals one. For sufficiently accurate simulations, the overlap depth must be considerably smaller than the radius of the particle

$$h_{\max} << R \tag{73}$$

This gives a criterion for the spring stiffness (Haff and Anderson (1993b))

$$k >> m \frac{v_{\max}^2}{R^2} \tag{74}$$

where v_{max} is the maximum possible value of relative contact velocity.

For Hooke's contact law ($\alpha = 1$) and with linear energy dissipation ($\eta \neq 0$, $\beta = 0$, $\lambda = 1$) under the condition of

$$\omega_\eta^2 = \omega^2 - \eta^2 > 0 \tag{75}$$

(otherwise the particles will lose all their kinetic energy in collision and not rebound), the law of particle motion will be

$$x = \frac{v_0}{\omega_\eta} \exp(-\eta t) \sin(\omega_\eta t) \tag{76}$$

$$v = \frac{v_0}{\omega_\eta} \exp(-\eta t)[\omega_\eta \cos(\omega_\eta t) - \eta \sin(\omega_\eta t)] \tag{77}$$

for the time $t < T_{c\eta}$, with $T_{c\eta}$ denoting the time of collision between two particles

$$T_{c\eta} = \frac{\pi}{\omega_\eta} = \frac{\pi}{\sqrt{\frac{k}{m} - \eta^2}} = \pi \sqrt{\frac{m}{k - m\eta^2}} \tag{78}$$

and the value of maximum overlap is expressed as

$$h_{\max} = \frac{v_0}{\omega_\eta} \exp(-\eta \tau) \sin(\omega_\eta \tau) \tag{79}$$

where

$$\tau = \frac{1}{\omega_\eta} arctg \frac{\omega_\eta}{\eta} \tag{80}$$

where τ is the time of maximum overlap. The coefficient of restitution, e, is expressed as

$$e = \left| \frac{v(T_{c\eta})}{v_0} \right| = \exp(-\eta T_{c\eta}) = \exp\left(\frac{-\eta \pi}{\omega_\eta} \right) \tag{81}$$

If the coefficient of restitution is known, the energy dissipation coefficient, η, can be calculated explicitly

$$\eta = -\frac{k}{m} \cdot \frac{\ln e}{\sqrt{\pi^2 + \ln^2 e}}$$

(82)

NON-LINEAR MODELS: For the Hertzian contact law ($\alpha = 3/2$), without energy dissipation ($\eta = 0$) and with an initial relative velocity of collision v_0, the collision time, T_c, can be expressed as (according to Landau and Lifshitz (1959))

$$T_c = 188 \left(\frac{25m_{ij}^2}{2k^2 v_0} \right)^{\frac{1}{5}} = 188 \left(\frac{25m_{ij}^2}{2k^2} \right)^{\frac{1}{5}} v_0^{-\frac{1}{5}}$$

(83)

The value of maximum overlap is expressed as

$$h_{\max} = \left(\frac{25m_{ij}^2}{2k^2} \right)^{\frac{1}{5}} v_0^{\frac{4}{5}}$$

(84)

The coefficient of restitution, e, equals one.

Taguchi (1992) showed that the Hertz contact model ($\alpha = 3/2$) with linear viscosity ($\beta = 0$, $\lambda = 1$), which was used by Lee and Herrmann (1993) contradicts the physical behaviour.

IV.3.3.2 Tangential Component of the Contact Force

To write a model for the tangential force is more difficult, as here the phenomena of tangential deformation and friction (static and dynamic) have to be modelled, whereas, in general, they depend on the normal force $\mathbf{F}_{n,ij}$ and displacement h_{ij} (equation (32) as well as on the history of the tangential contact force. The model of energy dissipation in tangential direction must also be included for static friction, because otherwise perpetual oscillations in the time of static friction will be obtained.

In literature, two major approaches can be found to model tangential forces: global models, where the tangential force is modelled by one law, and separated models, where static and dynamic friction are modelled by separate equations and Coulomb criteria.

GLOBAL MODELS. Mindlin (1949) and Mindlin and Deresiewicz (1953) developed a common theory for the tangential force which causes a small relative motion, which is called *slip*. Slip occurs in a partial area of contact, while the other part of contact remains adhered. When the tangential force $\mathbf{F}_{t,ij}$ increases, then the adhered area decreases to zero, which means that $\mathbf{F}_{t,ij}$ reaches a Coulomb-type cut-off limit. Then, sliding with friction occurs.

The most general development of the Mindlin and Deresiewicz theory was undertaken by Thornton and Yin (1991), where the general equations for tangential forces are derived. But this approach requires a very high computational expenditure and, therefore, mostly simplified expressions with assumptions of no partial slipping of the contact surface occurring are used. Walton and Braun (1986) approximated the expressions of Mindlin and Deresiewicz, where the effective tangential stiffness K_t is expressed by the equation

$$
K_t = \begin{cases} K_{t0}\left(1 - \dfrac{F_{t,ij} - F_{t,ij}^*}{\mu\, F_{n,ij} - F_{t,ij}^*}\right)^a & \Delta\delta_t \geq 0 \\[4mm] K_{t0}\left(1 - \dfrac{F_{t,ij}^* - \left(F_{t,ij}\right)^a}{\mu\, F_{n,ij} + F_{t,ij}^*}\right) & \Delta\delta_t < 0 \end{cases}
$$

(85)

where $\Delta\delta_t$ is the increment of the relative displacement between the contacting particles, K_{t0} is the initial tangential stiffness, μ is the dynamic friction coefficient, a is equal to 1/3 according to Mindlin's theory, $F_{t,ij}^*$ initially is zero and assumes the value of the total tangential force $\mathbf{F}_{t,ij}$, when $\Delta\delta_t$ changes the sign. When the normal force $\mathbf{F}_{n,ij}$ changes during contact, the value of $F_{t,ij}^*$ in equation (85) is scaled in proportion to the change in normal force. In each time step Δt, a new tangential force is calculated by the equation

$$
F_{t,ij}(t + \Delta t) = F_{t,ij}(t) + K_t(t)\Delta\delta_t(t)
$$

(86)

The model is in good agreement with the experimental data, which would even be better with a larger value of a. As obvious from Mindlin's theory, static and dynamic friction are modeled by the same equation (85) (Figure 19).

41
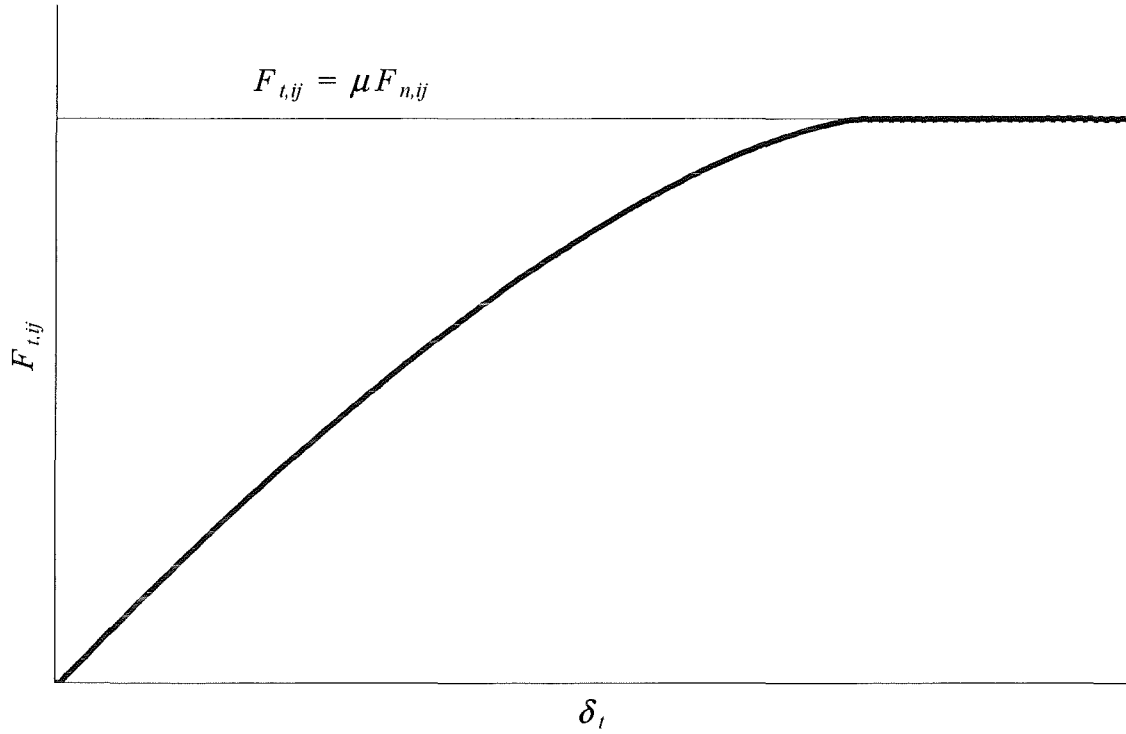
Figure 19. Mindlin and Deresiewicz (1953) model of tangential slip force, with $\Delta\delta_t > 0$ and $F^*_{t,ij} = 0$

The model used by Walton and Braun (1986) was also used by Sadd *et al.* (1993) with some modifications

$$K_t = \begin{cases} K_{t0}\left(1 - \dfrac{F_{t,ij} - F^*_{t,ij}}{\mu F_{n,ij} - F^*_{t,ij}}\right)^a & \Delta\delta_t \geq 0 \\[4mm] K_{t0}\left(1 - \dfrac{F^*_{t,ij} - F_{t,ij}}{\mu F_{n,ij} - F^*_{t,ij}}\right)^a & \Delta\delta_t < 0 \end{cases} \tag{87}$$

where K_{t0} and a are set to 5×10^5 N/m and 0.3, respectively. Lan and Rosato (1997) used the same model with $a = 1/3$ and $K_{t0} = 0.8K_1$, where $K_1 = 10^6$ N/m is the spring stiffness constant for the model of normal elastic force (equation (50)).

Chang *et al.* (1989) modified theory of the Hertz and Mindlin (1949) for two dimensional contacting cylinders and proposed a relationship for the tangential spring stiffness

$$K_{t,ij} = \frac{K_{n,ij}}{\Psi}\sqrt{1 - \frac{F_{t,ij}}{\tan\phi_\mu F_{n,ij}}} \tag{88}$$

where $K_{n,ij}$ is the normal spring stiffness and $F_{n,ij}$ is the normal force related by equations (48) and (49), Ψ is a constant, ϕ_μ is the friction angle between two contacting particles. For

$\Psi = 1$ (Chang *et al.* (1989)) the above equation is reduced to the equation proposed by Mindlin (1949).

SEPARATED MODELS. The most popular approach is where the evolution of tangential force $\mathbf{F}_{t,ij}$ can be divided into parts of static friction or dynamic friction occurring. *Dynamic friction force* can be described by the following equation:

$$\mathbf{F}_{t,ij,dynamic} = -\mu \left| \mathbf{F}_{n,ij} \right| \mathbf{t}_{ij} \tag{89}$$

where μ is the dynamic friction coefficient. When the tangential force $\mathbf{F}_{t,ij}$ is larger then the Coulomb-type cut-off limit, dynamic friction acts. When $\mathbf{F}_{t,ij}$ is lower than the limit, the model of static friction force $\mathbf{F}_{t,ij,static}$ must be implemented. Such an approach can be modelled by

$$\mathbf{F}_{t,ij} = \begin{cases} \mathbf{F}_{t,ij,static} & for \left| \mathbf{F}_{t,ij,static} \right| < \left| \mathbf{F}_{t,ij,dynamic} \right| \\ \mathbf{F}_{t,ij,dynamic} & for \left| \mathbf{F}_{t,ij,static} \right| \geq \left| \mathbf{F}_{t,ij,dynamic} \right| \end{cases} \tag{90}$$

or, in a more convenient form for programming

$$\mathbf{F}_{t,ij} = -\mathbf{t}_{ij} \min\left(\left| \mathbf{F}_{t,ij,static} \right|, \left| \mathbf{F}_{t,ij,dynamic} \right| \right) \tag{91}$$

where $\mathbf{t}_{ij}$ is the unit vector of the tangential direction of the contact point. Below, models of *static friction force* are be discussed only.

The expression (89) of the dynamic friction force is clear, but there is no common agreement on the model for static friction. The most popular approach is based on the assumption that static friction can be calculated by the sum of energy dissipation and spring models

$$\mathbf{F}_{t,ij,static} = \mathbf{F}_{t,ij,spring} + \mathbf{F}_{t,ij,dissipation} \tag{92}$$

The spring model was proposed by Lee and Herrmann (1993). The most general form of the spring model for static friction was used by Kohring (1995) and Kohring (1996) in simplified expressions of Mindlin's theory, assuming that no partial slipping of the contact surface occurs

$$\mathbf{F}_{t,ij,spring} = -k_{t,ij} \delta_{t,ij} \mathbf{t}_{ij} \tag{93}$$

where $\delta_{t,ij}$ is the integrated slip in the tangential direction after the particles i and j came into contact and defined by (10). $\delta_{t,ij}$ is allowed to increase until the tangential force exceeds the limit imposed by static friction. $k_{t,ij}$ is the spring stiffness constant and expressed by

$$k_{t,ij} = \frac{16}{3} \cdot \frac{G_i G_j \sqrt{R_{ij} h_{ij}}}{G_i \left(2 - \sigma_j \right) + G_j \left(2 - \sigma_i \right)} \tag{94}$$

where G_i is the shear modulus of the material. This model does not require such a high computational expenditure than the model of Walton and Braun (1986) (equation (85)), however, the qualitative results appear to be the same (Kohring (1995)). Lin and Ng (1997)

used a model similar to (93) and (94) with some modifications for simulating the contact between ellipsoids.

For particles of the same material, Dury and Ristow (1997), Lee and Herrmann (1993) Khakhar et al. (1997) used a simpler constant spring model for the static force in the equation (93), where $k_{t,ij} = const.$

It is evident that the model of static friction (93) does not approximate the energy dissipation during static friction as accurate as it is modelled by (85) or (87). For this purpose, the model for energy dissipation in tangential direction can be used (Thompson and Grest (1991), Haff and Werner (1986), Lee and Herrmann (1993), Ristow (1994b)), as in the model for energy dissipation in the normal direction (60)

$$\mathbf{F}_{t,ij,dissipation} = -\gamma_t m_{ij} \mathbf{v}_{t,ij} \qquad (95)$$

where γ_t is the shear dissipation coefficient and m_{ij} is the effective mass expressed by equation (61).

MODELS OF TANGENTIAL FORCES FOR CONTINUOUS INTERACTION. Langston et al. (1994) and Langston et al. (1995) adopted the theory of Mindlin and derived an equation for friction with the normal force described by continuous interaction models using equation (57).

$$F_{t,ij} = \mu F_{n,ij} \left[1 - \left(1 - \frac{|\delta_{t,ij}|}{\delta_{t,ij,max}} \right)^{3/2} \right] \qquad (96)$$

where

$$\delta_{t,ij,max} = C_t \mu F_{n,ij} \qquad (97)$$

C_t is the average tangential compliance. If $|\delta_{t,ij}| > \delta_{t,ij,max}$, then $|\delta_{t,ij}| = \delta_{t,ij,max}$, which means that sliding occurs and $\delta_{t,ij}$ does not increase.

IV.3.3.2.1 Discussion of Tangential Forces

As above-mentioned, there is no agreement on which model is best suited. Various combinations of forces are used by authors, depending on the requirements regarding low cost and the accuracy of numerical simulation. For example:

- Several authors (*e.g.* Poschel and Buchholtz (1993), Gallas and Sokolowski (1993), Kohring et al. (1995)) only used equation (95) to simulate static friction

$$\mathbf{F}_{t,ij,static} = \mathbf{F}_{t,ij,dissipation} \qquad (98)$$

- Some authors (*e.g.* Khakhar et al. (1997)) only used the spring model (equation (93)) to simulate static friction

$$\mathbf{F}_{t,ij,static} = \mathbf{F}_{t,ij,spring} \qquad (99)$$

44

- Some authors (*e.g.* Lee and Herrmann (1993), Tsuji *et al.* (1993), Taguchi (1992b)) only used the static friction model to simulate friction without implementation of a dynamic friction model

$$\mathbf{F}_{t,ij} = \mathbf{F}_{t,ij,static} \qquad (100)$$

- In general, tangential coefficients of spring stiffness and dissipation are different from normal ones, but Tsuji *et al.* (1993) and Taguchi (1992b) modelled shear forces only by using the same linear model as for normal elastic contact and energy dissipation with the same stiffness and viscosity coefficients k and γ, respectively

$$\mathbf{F}_{ij}^t = -kh_{ij}\mathbf{t}_{ij} - \gamma\,\mathbf{v}_{ij}^t \qquad (101)$$

- Akiyama *et al.* (1996) only used the model of shear dissipation forces for tangential forces in the continuous interaction model

$$\mathbf{F}_{t,ij} = \mathbf{F}_{t,ij,dissipation} \qquad (102)$$

IV.3.3.3 General Discussions of Forces

Ristow (1992) investigated the continuous interaction and Hertzian normal force models and concluded that some phenomena of granular flow (e.g. arching) were described more accurately by the second model. But the continuous interaction model had been used without shear forces. Furthermore, both models did not include rotation, which might have played a crucial role (Ristow (1992)).

Langston *et al.* (1995) and Langston *et al.* (1995b) compared three forms of normal interaction - Hooke's law, Hertzian and continuous interaction. They concluded that some effects, such as the internal flow patterns and the distribution of the high shear region significantly depend on the choice of the particle interaction type. However, the internal distribution of the bulk normal stress is affected very little by this choice (Langston *et al.* (1995b)). The major advantage of the continuous interaction model developed by them is that it allows to simulate with sufficient accuracy over much longer time periods using time steps of the order of 10^{-5} s in comparison to 10^{-7}-10^{-9} s of other models, while maintaining the essential physics of interparticle and particle-wall interaction (Langston *et al.* (1994)). Continuous interaction models, which give rise to prolonged frictional engagement at very small contact normal loads appear to yield a much more realistic bulk flow in hoppers than those that scale shear strains in direct proportion to the magnitude of normal loads, such as Hertz law (Langston *et al.* (1995b)).

Sadd *et al.* (1993) investigated linear (equations (37) and (38)), non-linear (equation (45)) with $\alpha = 1.4$ and the non-linear hysteresis law (equation (53)) normal force-deformation contact models. All three normal contact models were used in simulations of the wave behaviours of propagation including wave attenuation and dispersion characteristics. Numerical results were compared with experimental data for a simple geometry of single disk chains (one-dimensional case). The linear contact law with the normal linear energy dissipation (equation (57)) produces an unreasonably high dispersion of wave form spreading in comparison with the experiments. Non-linear contact models without energy reduced this excess dispersion, however, the dispersion again became unacceptably high when the model of energy dissipation was added. The non-linear hysteresis law provides damping by itself. The results of simulation with the stiffness hysteresis law and without any additional energy dissipation model were in the best agreement with the experiments for wave speeds and amplitude attenuation and predicted the proper dispersion characteristics observed in the experiments (Sadd *et al.* (1993)). Two-dimensional granular assemblies were simulated by using the non-linear normal contact model with the modified model of Walton and Braun (equation (87)) for tangential contact forces. The average relative errors between the experimental and the predicted values were less than 15%.

IV.3.4 Problems of Rotation

ONE-DIMENSIONAL motion of particles is without rotation. In this case, we do not need to solve equations of orientation.

Orientation θ, angular velocity w, angular acceleration u, torques T and inertia momentum I of *TWO-DIMENSIONAL* particles can be treated as scalars. Therefore, the equations of rotation (26) and (27) for two-dimensional particles can be simplified as follows

$$I_i \frac{d^2\theta_i}{dt^2} = I_i u_i = T_i \qquad (103)$$

$$w_i = \frac{d\theta_i}{dt} \qquad (104)$$

For *THREE-DIMENSIONAL* particles, however, the inertia moment must be calculated in every time step according to the new orientation of the particle in space. Therefore, it is convenient to use two coordinate systems: a fixed in a space laboratory - space-fixed or laboratory coordinate system, and a moving Cartesian coordinate system which is fixed with the particle and whose axes are the principal axes of inertia - body-fixed or local coordinate system (Rahman and Stillinger (1971)). Then, the inertia tensor is always diagonal $I_i = (I_{1i}, I_{2i}, I_{3i})$ in a body-fixed coordinate system. For spherical particles, $I_{1i} = I_{2i} = I_{3i} = I_i$ and body-fixed coordinates can be set in the same direction as space-fixed ones. Therefore, orientation is not used for spheres and the equations of rotation (26) and (27) can be rewritten in a simpler form

$$\frac{d\mathbf{w}_i}{dt} = \frac{\mathbf{T}_i}{I_i} \qquad (105)$$

The rotation of three-dimensional particles with arbitrary shapes may be defined by Euler angles. 12 independent definitions of Euler angles can be given. The most popular ones are *x-convention* (rotate about z, x', z''), *y-convention* (rotate about z, y', z''), *xyz-convention* (rotate about x, y', z''). The latter is used for engineering applications and referred to as *Tait-Bryan* angles (Goldstein (1980)). Here, we will use *x-convention*. More details on other conventions can be found in Goldstein (1980).

If we denote this molecule-fixed system by primes, then transformation of any vector $\mathbf{v}$ from the space-fixed axes $\mathbf{v}^s$ to the body-fixed axes $\mathbf{v}^b$ and *vice versa* can be made as (Goldstein (1980) and Allen and Tildesley (1990))

$$\mathbf{v}^b = \mathbf{A} \cdot \mathbf{v}^s \qquad (106)$$

$$\mathbf{v}^s = \mathbf{A}^{-1} \cdot \mathbf{v}^b \qquad (107)$$

where the transformation matrix is the same matrix of body axis rotation by Euler angles (ϕ, θ, ψ):

$$
\mathbf{A} = \begin{pmatrix} \cos\phi\cos\psi - \sin\phi\cos\theta\sin\psi & \sin\phi\cos\psi + \cos\phi\cos\theta\sin\psi & \sin\theta\sin\psi \\ -\cos\phi\sin\psi - \sin\phi\cos\theta\cos\psi & -\sin\phi\sin\psi + \cos\phi\cos\theta\cos\psi & \sin\theta\cos\psi \\ \sin\phi\sin\theta & -\cos\phi\sin\theta & \cos\theta \end{pmatrix} \qquad (108)
$$

If the vector $\mathbf{v}$ is fixed in the body frame, then the change of $\mathbf{v}^b$ with time will be different from the changes of $\mathbf{v}^s$

$$
\left(\frac{d\mathbf{v}}{dt}\right)^s = \left(\frac{d\mathbf{v}}{dt}\right)^b + \left[\mathbf{w}^s \times \mathbf{v}^s\right] \qquad (109)
$$

Then, the corresponding torque components in the body-fixed coordinate system are

$$
\mathbf{T}_i^b = \left(T_{ix'}^b, T_{iy'}^b, T_{iz'}^b\right) \qquad (110)
$$

The same components must obey the Euler equations:

$$
\frac{d\mathbf{M}_i^b}{dt} + \left[\mathbf{w}_i^b \times \mathbf{M}_i^b\right] = \mathbf{T}_i^b \qquad (111)
$$

or

$$
I_1 \frac{dw_{ix'}^b}{dt} - w_{iy'}^b w_{iz'}^b \left(I_2 - I_3\right) = T_{ix'}^b
$$

$$
I_2 \frac{dw_{iy'}^b}{dt} - w_{iz'}^b w_{ix'}^b \left(I_3 - I_1\right) = T_{iy'}^b \qquad (112)
$$

$$
I_3 \frac{dw_{iz'}^b}{dt} - w_{ix'}^b w_{iy'}^b \left(I_1 - I_2\right) = T_{iz'}^b
$$

where $\mathbf{M}_i$ is the total angular momentum of the particle. The angular velocity components in the body-fixed coordinate system can be represented as follows in terms of the Euler angles:

$$
w_{ix'}^b = \frac{d\phi_i}{dt}\sin\theta_i \sin\psi_i + \frac{d\theta_i}{dt}\cos\psi_i
$$

$$
w_{iy'}^b = \frac{d\phi_i}{dt}\sin\theta_i \cos\psi_i - \frac{d\theta_i}{dt}\sin\psi_i \qquad (113)
$$

$$
w_{iz'}^b = \frac{d\phi_i}{dt}\cos\theta_i + \frac{d\psi_i}{dt}
$$

or in space-fixed coordinates:

$$
\mathbf{w}_i^s = \mathbf{A}^{-1} \cdot \mathbf{w}_i^b \qquad (114)
$$

or

48

$$w_{ix}^s = \frac{d\theta_i}{dt}\cos\phi_i + \frac{d\psi_i}{dt}\sin\theta_i\sin\phi_i$$

$$w_{iy'}^s = \frac{d\theta_i}{dt}\sin\phi_i - \frac{d\psi_i}{dt}\sin\theta_i\cos\phi_i \qquad (\,115\,)$$

$$w_{iz'}^s = \frac{d\psi_i}{dt}\cos\theta_i + \frac{d\phi_i}{dt}$$

Now, we can calculate the changes of the Euler angles during impact from the equations of

$$\frac{d\phi_i}{dt} = \frac{w_{ix'}^b \sin\psi_i + w_{iy'}^b \cos\psi_i}{\sin\theta_i}$$

$$\frac{d\theta_i}{dt} = w_{ix'}^b \cos\psi_i - w_{iy'}^b \sin\psi_i \qquad (\,116\,)$$

$$\frac{d\psi_i}{dt} = w_{iz'}^b - \left(w_{ix'}^b \sin\psi_i + w_{iy'}^b \cos\psi_i\right)\frac{\cos\theta_i}{\sin\theta_i}$$

or

$$\frac{d\phi_i}{dt} = \left(-w_{ix}^s \sin\phi_i + w_{iy}^s \cos\phi_i\right)\frac{\cos\theta_i}{\sin\theta_i} + w_{iz}^s$$

$$\frac{d\theta_i}{dt} = w_{ix}^s \cos\psi_i + w_{iy}^s \sin\psi_i \qquad (\,117\,)$$

$$\frac{d\psi_i}{dt} = \frac{w_{ix}^s \sin\phi_i - w_{iy}^s \cos\phi_i}{\sin\theta_i}$$

Unfortunately, the equations of motion (116) or (117) will contain singularities at Euler's angle θ near $\{0, \pi\}$. Thus, Euler's angles are not convenient for describing the full rotation of particles. According to Ciccotti (1987, pp. 325-326), there are at least three methods to solve this problem:

1. Rahman and Stillinger (1971), Barojas *et al.* (1973) and Levesque *et al.* (1983) used the modified Euler-angle approach to redefine the coordinate frame when $\sin\theta$ becomes dangerously small, *i.e.* two alternative sets of body-fixed axes were used for each particle and whenever the angle θ was near $\{0, \pi\}$, then another set was used for the calculations. Details of the method were first given in a paper by Barojas *et al.* (1973).

2. Ciccotti *et al.* (1982) proposed a method of constraints, in which the equations of motion are solved in Cartesian form. The method of constraints is easily applicable to systems of flexible molecules (Ciccotti (1987)).

3. Evans and Murad (1977) and Evans (1977) proposed another approach that involves a transformation from Eulerian angles to a set of quaternions, which are also known as

49

Euler's four parameters according to Fan and Ahmadi (1995)). This method will be shortly described below.

All methods are of similar computational efficiency (Ciccotti (1987), see notes in pp. 326 and 372), but methods of constraints and quaternions are the most commonly used schemes.

Methods of quaternions. The description of the method can be found in Evans and Murad (1977), Evans (1977), Fincham and Heyes (1985), Goldstein (1980), Hughes (1986), Allen and Tildesley (1990) and Fan and Ahmadi (1995).

A quaternion for each particle i is a set of four scalars $\mathbf{Q}_i = (q_{i0}, q_{i1}, q_{i2}, q_{i3})$ which must satisfy the constraint equation of

$$\sum_j q_{ij}^2 = 1 \qquad (118)$$

We can define the quaternion as

$$q_0 = \cos\tfrac{1}{2}\theta \cos\tfrac{1}{2}(\phi + \psi)$$

$$q_1 = \sin\tfrac{1}{2}\theta \cos\tfrac{1}{2}(\phi - \psi)$$

$$q_2 = \sin\tfrac{1}{2}\theta \sin\tfrac{1}{2}(\phi - \psi) \qquad (119)$$

$$q_3 = \cos\tfrac{1}{2}\theta \sin\tfrac{1}{2}(\phi + \psi)$$

Then, the rotation matrix (108) of a body-fixed frame in a space-fixed frame can be expressed as

$$\mathbf{A} = \begin{pmatrix} q_0^2 + q_1^2 - q_2^2 - q_3^2 & 2(q_1 q_2 + q_0 q_3) & 2(q_1 q_3 - q_0 q_2) \\ 2(q_1 q_2 - q_0 q_3) & q_0^2 - q_1^2 + q_2^2 - q_3^2 & 2(q_2 q_3 + q_0 q_1) \\ 2(q_1 q_3 + q_0 q_2) & 2(q_2 q_3 - q_0 q_1) & q_0^2 - q_1^2 - q_2^2 + q_3^2 \end{pmatrix} \qquad (120)$$

and the time derivatives of the quaternions are obtained for each particle

$$\begin{pmatrix} \dot{q}_{i0} \\ \dot{q}_{i1} \\ \dot{q}_{i2} \\ \dot{q}_{i3} \end{pmatrix} = \frac{1}{2} \begin{pmatrix} q_{i0} & -q_{i1} & -q_{i2} & -q_{i3} \\ q_{i1} & q_{i0} & -q_{i3} & q_{i2} \\ q_{i2} & q_{i3} & q_{i0} & -q_{i1} \\ q_{i3} & -q_{i2} & q_{i1} & q_{i0} \end{pmatrix} \begin{pmatrix} 0 \\ w_{ix}^b \\ w_{iy}^b \\ w_{iz}^b \end{pmatrix} \qquad (121)$$

or

$$\dot{q}_{i0} = -\frac{1}{2}\left(q_{i1} w_{i1}^b + q_{i2} w_{i2}^b + q_{i3} w_{i3}^b\right)$$

$$\dot{q}_{i1} = \frac{1}{2}\left(q_{i0} w_{i1}^b - q_{i3} w_{i2}^b + q_{i2} w_{i3}^b\right)$$

$$\dot{q}_{i2} = \frac{1}{2}\left(q_{i3}w_{i1}^b + q_{i0}w_{i2}^b - q_{i1}w_{i3}^b\right)$$
(122)

$$\dot{q}_{i3} = \frac{1}{2}\left(-q_{i2}w_{i1}^b + q_{i1}w_{i2}^b + q_{i0}w_{i3}^b\right)$$

It is possible to keep in the memory only three quaternions, because the fourth can be calculated from the constraint equation (118).

IV.4 TIME INTEGRATION

The time step, Δt, for the time integration of the particle position, velocity, orientation and angular velocity (equations (18), (19), (26) and (27)) depends on the time of contact T_c which is described in section on normal contact forces on page 38. Two main criteria are applied to a time step:

1) The time step must be small enough to ensure a stable numerical scheme of time integration. Cundall and Strack (1979) proposed that the time step must be smaller than the critical time step, Δt_c,

$$\Delta t_c = \sqrt{\frac{m}{k}}$$

(123)

which was estimated on the basis of the single degree-of-freedom system of a mass m connected to the ground by a spring of stiffness k.

2) The time step must be considerably smaller than the contact time T_c in order to correctly simulate the behaviour of granular media. In spite of the assertion of Thompson and Grest (1991) that an accurate simulation requires $\Delta t \sim T_c/50$, other authors use a larger time step, for example, Dury and Ristow (1997) used $\Delta t = T_c/15$ and Ristow (1996b) - $\Delta t = T_c/10$, Langston $et\ al.$ (1995) - $\Delta t \sim T_c/30$.

See Haff and Anderson (1993b) for more details on the time scales criterion of the time step and Langston $et\ al.$ (1994) and Langston $et\ al.$ (1995) for the time scales of continuous interaction model.

Various integration schemes can be used, but according to Sundaram and Collins (1996) the third-order accuracy is required at a minimum to accurately track the particle trajectories. The Verlet scheme and the fifth order Gear predictor corrector are the most popular schemes used to integrate the equations (18), (19), (26) and (27). These schemes are described in detail by Allen and Tildesley (1990).

Some of the most popular schemes used in DEM will be presented.

The **PREDICTOR-CORRECTOR** scheme with the Newmark parameters (Newmark 1959) $\alpha = 0.5$ and $\beta = 0.25$ for the predictor stage

$$\mathbf{x}^p(t + \Delta t) = \mathbf{x}(t) + \Delta t \mathbf{v}(t) + \frac{1}{2}\Delta t^2(1 - 2\beta)\mathbf{a}(t)$$

$$\mathbf{v}^p(t + \Delta t) = \mathbf{v}(t) + \frac{1}{2}\Delta t(1 - \alpha)\mathbf{a}(t)$$

(124)

for the force balance after the predictor stage,

$$\mathbf{a}^p(t + \Delta t) = \frac{\mathbf{F}^p(\mathbf{x}^p, \mathbf{v}^p)}{m}$$

(125)

and for the corrector stage

$$\begin{pmatrix} \mathbf{x}^c(t+\Delta t) \\ \mathbf{v}^c(t+\Delta t) \end{pmatrix} = \begin{pmatrix} \mathbf{x}^p(t+\Delta t) \\ \mathbf{v}^p(t+\Delta t) \end{pmatrix} + \begin{pmatrix} \Delta t^2 \beta \\ \Delta t \alpha \end{pmatrix} \mathbf{a}^p(t+\Delta t)$$

(126)

was used by Xu and Yu (1997).

The **FOURTH-ORDER HERMITE PREDICTOR-CORRECTOR** scheme was used by Makino *et al.* (1993). The predictor is expressed as

$$\mathbf{x}^p(t+\Delta t) = \mathbf{x}(t) + \Delta t \mathbf{v}(t) + \frac{1}{2}\Delta t^2 \mathbf{a}(t) + \frac{1}{6}\Delta t^3 \dot{\mathbf{a}}(t)$$

$$\mathbf{v}^p(t+\Delta t) = \mathbf{v}(t) + \Delta t \mathbf{a}(t) + \frac{1}{2}\dot{\mathbf{a}}(t)$$

(127)

with predicted acceleration and its derivative as

$$\mathbf{a}^p(t+\Delta t) = f\left(\mathbf{x}^p, \mathbf{v}^p\right)$$

(128)

$$\dot{\mathbf{a}}^p(t+\Delta t) = f\left(\mathbf{x}^p, \mathbf{v}^p, \mathbf{a}^p\right)$$

Then, the corrector is given by the following formula

$$\mathbf{x}^c(t+\Delta t) = \mathbf{x}(t) + \frac{1}{2}\Delta t\left[\mathbf{v}^p(t+\Delta t) + \mathbf{v}(t)\right] - \frac{1}{12}\Delta t^2\left[\mathbf{a}^p(t+\Delta t) - \mathbf{a}(t)\right]$$

(129)

$$\mathbf{v}^c(t+\Delta t) = \mathbf{x}(t) + \frac{1}{2}\Delta t\left[\mathbf{a}^p(t+\Delta t) + \mathbf{a}(t)\right] - \frac{1}{12}\Delta t^2\left[\dot{\mathbf{a}}^p(t+\Delta t) - \dot{\mathbf{a}}(t)\right]$$

The third-order **GEAR PREDICTOR-CORRECTOR** scheme was used by Thompson and Grest (1991). The fifth order scheme was used by Lee and Herrmann (1993), Form *et al.* (1993), Gallas *et al.* (1992), Kalthoff *et al.* (1996). Here, a short description of the Gear predictor-corrector scheme is given.

At first, the positions, velocities and higher order of time derivatives up to the desired order of accuracy are predicted by

$$\mathbf{x}^p(t+\Delta t) = \mathbf{x}(t) + \Delta t \mathbf{v}(t) + \frac{1}{2}\Delta t^2 \mathbf{a}(t) + \frac{1}{6}\Delta t^3 \mathbf{b}(t) + \dots$$

(130)

$$\mathbf{v}^p(t+\Delta t) = \mathbf{v}(t) + \Delta t \mathbf{a}(t) + \frac{1}{2}\Delta t^2 \mathbf{b}(t) + \dots$$

$$\mathbf{a}^p(t+\Delta t) = \mathbf{a}(t) + \Delta t \mathbf{b}(t) + \dots$$

$$\mathbf{b}^p(t+\Delta t) = \mathbf{b}(t) + \dots$$

53

After the prediction, the particle forces and accelerations are calculated according to the new positions and velocities

$$\mathbf{a}^c(t+\Delta t) = \frac{\mathbf{F}^p(\mathbf{x}^p, \mathbf{v}^p)}{m}$$

(131)

Then, the positions, velocities and higher-order time derivatives are corrected

$$\Delta\mathbf{a}(t+\Delta t) = \mathbf{a}^c(t+\Delta t) - \mathbf{a}^p(t+\Delta t)$$

(132)

$$\begin{pmatrix} \mathbf{x}^c(t+\Delta t) \\ \mathbf{v}^c(t+\Delta t) \\ \mathbf{a}^c(t+\Delta t) \\ \mathbf{b}^c(t+\Delta t) \\ \dots \end{pmatrix} = \begin{pmatrix} \mathbf{x}^p(t+\Delta t) \\ \mathbf{v}^p(t+\Delta t) \\ \mathbf{a}^p(t+\Delta t) \\ \mathbf{b}^p(t+\Delta t) \\ \dots \end{pmatrix} + \begin{pmatrix} c_0 \\ c_1 \\ c_2 \\ c_3 \\ \dots \end{pmatrix} \Delta\mathbf{a}(t+\Delta t)$$

(133)

The values of the constants c_i depend on the desired accuracy, and for a second order of differential equation

$$\frac{d^2\mathbf{r}}{dt^2} = f\left(\mathbf{r}, \frac{d\mathbf{r}}{dt}\right)$$

(134)

are $c_0 = 3/16$, $c_1 = 251/360$, $c_2 = 1$. $c_3 = 11/18$, $c_4 = 1/6$ and $c_5 = 1/60$ (Allen and Tildesley (1990)).

EULER'S scheme of

$$\mathbf{x}(t+\Delta t) = \mathbf{x}(t) + \mathbf{v}(t)\Delta t$$

$$\mathbf{v}(t+\Delta t) = \mathbf{v}(t) + \mathbf{a}(t)\Delta t$$

(135)

was used by Taguchi (1992b), Sadd *et al.* (1993), Tsuji *et al.* (1992) and Tsuji *et al.* (1993).

The scheme of TAYLOR EXPANSION SERIES up to acceleration

$$\mathbf{x}(t+\Delta t) = \mathbf{x}(t) + \mathbf{v}(t)\Delta t + \frac{1}{2}\mathbf{a}(t)\Delta t^2$$

$$\mathbf{v}(t+\Delta t) = \mathbf{v}(t) + \mathbf{a}(t)\Delta t$$

(136)

was used by Taguchi (1992).

The VELOCITY VERLET scheme

$$\mathbf{x}(t+\Delta t) = \mathbf{x}(t) + \mathbf{v}(t)\Delta t + \frac{1}{2}\mathbf{a}(t)\Delta t$$

$$v(t + \Delta t) = v(t) + \frac{1}{2}[a(t) + a(t + \Delta t)]\Delta t \qquad (137)$$

was used by Aoki and Akiyama (1995), Kopf *et al.* (1997) and Satoh (1995). Furthermore, it was also investigated by Satoh (1995b).

The **HALF-STEP LEAP-FROG VERLET** scheme

$$x(t + \Delta t) = x(t) + v(t + \Delta t/2)\Delta t$$

$$v(t + \Delta t/2) = v(t - \Delta t/2) + a(t)\Delta t \qquad (138)$$

was used by Langston *et al.* (1994), Langston *et al.* (1995) and Lan and Rosato (1997). This scheme cannot be used directly for the rotation by quaternions, because the quaternion derivatives do not only depend on the angular velocity, but also on Q itself (Allen and Tildesley (1990).

The **SECOND-ORDER ADAMS-BASHFORTH** scheme

$$x(t + \Delta t) = x(t) + \frac{1}{2}[3v(t) - v(t - \Delta t)]\Delta t$$

$$v(t + \Delta t) = v(t) + \frac{1}{2}[3a(t) - a(t - \Delta t)]\Delta t \qquad (139)$$

was used by Sundaram and Collins (1996).

The **FOURTH-ORDER RUNGE-KUTTA** scheme was used by Ovensen *et al.* (1996) for Molecular Dynamics.

The Gear predictor-corrector scheme is described in details by van Gunsteren and Berendsen (1977) and Allen and Tildesley (1990). Van Gunsteren and Berendsen (1977) applied and compared Gear predictor-corrector and Verlet schemes for macromolecular dynamics applications and obtained the best results with the Gear scheme.

Darmorfal and Haimes (1996) investigated algorithms of path integration of massless particles in a steady and unsteady velocity vector field, for example, in a surrounding fluid. They analysed the relative stability and accuracy of the following schemes: second-order, single-stage Adams-Moulton or trapezoidal integration; fourth-order backwards differentiation (BD4); fourth-order Adams-Bashforth and fourth-order Runge-Kutta (RK4). It was shown that many multi-stage and multi-step schemes were limited to third-order accuracy due to start-up errors. Only BD4 and RK4 performed well. An advantage of the BD4 scheme is that only the current velocity field needs to be stored in the memory, while the RK4 scheme requires to store four velocity fields. However, the RK4 schemes are the most accurate schemes tested. Another important conclusion was that the maximum time step must be of the order of the physical time-scale of unsteady flow to ensure accurate integrations of the particle path in the velocity fields.

Shida *et al.* (1997) investigated the numerical error of total energy for a conservative system of particles with linear and non-linear inter-particle forces. They found that the fourth-order Runge-Kutta scheme yields a fifth order accuracy for the total energy.

Satoh (1995b) and Satoh (1997) investigated the velocity Verlet, the half-step leap-frog Verlet scheme, the Beeman scheme, the four-value Gear predictor-corrector and some modified Beeman and Verlet schemes for the conservative system of continuous interaction of inter-particle forces (Lennard-Jones 12-6 potential). The results were that the velocity Verlet algorithm was the best scheme. It was followed by the leap-frog scheme and by the Beeman scheme. The four-value Gear predictor-corrector exhibited the worst performance in terms of stability and energy fluctuation.

Kopf *et al.* (1997) proposed a multiple time step integrator for Hamiltonian systems with disparate masses, which conserves energy. This method was proposed for molecular dynamics, and it would be difficult to apply it for the simulation of granular material. Perhaps it would be applicable to some kinds of flow of granular material.

An interesting generalised Gear fourth order predictor-corrector scheme was developed by Ariel (1997) to obtain the numerical solution of a class of singular boundary value problems. Possible applications of this scheme for the simulation of particle motion requires more detailed studies.

V. PROGRAMMING

V.1 OBJECT-ORIENTED PROGRAMMING

The decision for the implementation of a granular material model into computer code is a choice of programming methodology and language. Two major approaches are used today: methodologies of structured programming languages and Object-Oriented Programming.

FORTRAN is the most popular structured programming language for scientific calculations. The C programming language is the popular for system and user interface programming. However, the methodology of structured languages such as C and FORTRAN do not provide flexible mechanisms for software extension (Verboncoeur *et al.* (1995) and Peters (1996)).

An alternative used to model the processes of the real world is the Object-Oriented Programming (OOP) methodology (Peters (1996)). The real word consists of entities interacting with each other. The software model reproduces entites of the real word by objects, which communicate with each other through messages (Figure 20). Therefore, Object-Oriented Programming is a natural choice for the simulation of the behaviour of granular material, where particles obviously correspond to objects. Another advantage of the OOP is the flexible software development process. As a consequence, the object-oriented methodology is chosen to suit best the needs for the simulation of granular material behaviour.
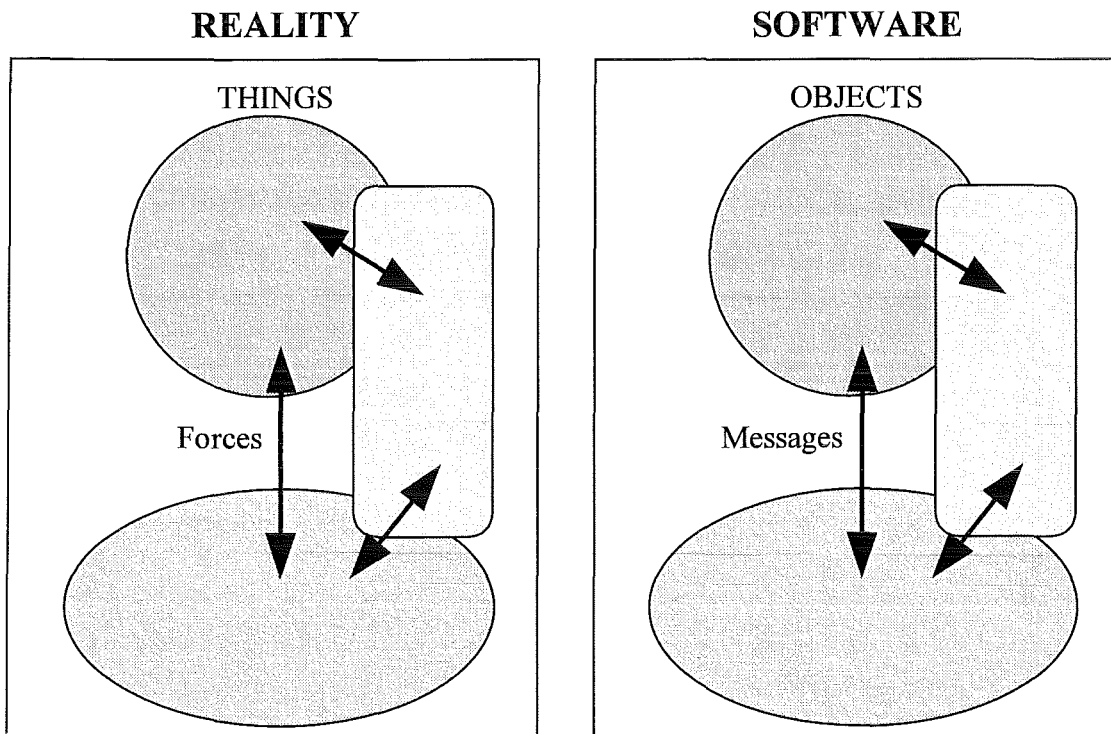
Figure 20. Object-Oriented Programming (OOP) methodology

The simulation method used for this application is designed on the basis of the OOM and is programmed in the programming language C++ (Stroustrup (1991)). This approach supports objects that can be used for three-dimensional particles of various shapes and sizes as well as

57

for the walls as boundaries of simulation area. The programming code is implemented in the TOSCA software package (Tools of Object-oriented Software for Continuum mechanic Applications), which allows for a high degree of flexibility and for the shortening the software development process (Peters (1996) and Peters (1997)).

The OOP methodology is used to program a particles-in-cells code for simulating plasmas (Verboncoeur *et al.* (1995)). A further application of the OOP methodology consists of classes to numerically solve problems of plasma physics, suspension flow, vortex simulations, porous media and material science (Reynders *et al.* (1995)). It was found that the FORTRAN version ran about twice as fast as the comparable C++ version (see Verboncoeur *et al.* (1995)). But this comparison was made at least seven years ago, and it is believed that nowadays compilers of C++ are faster and extensions of the C++ language will yield a much faster code. This belief, however, remains to be confirmed by new investigations of the comparable code programmed by FORTRAN and C++. The same investigation must be made for the criteria of code paralellization and vectorization, because it may be crucial for the speed of the code.

Options of OOP development for molecular dynamics simulations on the parallel computers were discussed by Baekdal *et al.* (1996). The software used for our applications, however, does momentarily not include paralellization and vectorization. But it is going to be implemented in the next stage of software development.

V.2 NEIGHBORS-SEARCH ALGORITHM

At each time step, the contact overlap of each particle with its neighbours must be found. The straightforward method gives the total number of calculations for a granular material consisting of N particles

$$C_{total} = \sum_{k=1}^{N}(N-k) \approx \frac{N^2}{2} \qquad (\mathbf{140})$$

It is an the order of $O(N^2)$. In literature, some effective neighbors-search algorithms (NSA) can be found to reduce C_{total} to $O(N \log N)$ or $O(N)$ (e.g. Williams and O'Connor (1995) for two-dimensional problems).

VI. SIMULATION

VI.1 METHOD

The time-driven method was used to simulate the behaviour of granular material, which means that an impact between particles is approximated by a representative overlap area or volume of particle shapes in the vicinity of the point of impact. The state of all particles, at the time t, are updated after fixed time step Δt, which is smaller than the smallest time of impact. The motion of each particle in the granular material is described by the second Newton law

$$m_i \frac{d^2 \mathbf{x}_i}{dt_2} = m_i \mathbf{a}_i = \mathbf{F}_i \tag{141}$$

$$\mathbf{v}_i = \frac{d\mathbf{x}_i}{dt} \tag{142}$$

$$I_i \frac{d\mathbf{w}_i}{dt} = \mathbf{T}_i \tag{143}$$

where $\mathbf{v}_i$, $\mathbf{a}_i$, $\mathbf{x}_i$, $\mathbf{w}_i$ are vectors of velocity, acceleration, position and angular velocity of the centre of gravity m_i of the particle i ($i = [1, N]$), N is the number of particles in the granular material. I_i is the inertial tensor of the particle. $\mathbf{F}_i$ and $\mathbf{T}_i$ are the sum of all forces and torques, respectively, which act on the particle i. External forces and the fluid influence were neglected. Therefore, $\mathbf{F}_i = \mathbf{F}_{i,contact}$ and $\mathbf{T}_i = \mathbf{T}_{i,contact}$, where $\mathbf{F}_{i,contact}$ is the summation of direct contact forces between the particle i and another N - 1 particle

$$\mathbf{F}_{i,contact} = \sum_{j=1, j \neq i}^{N} \mathbf{F}_{ij} \tag{144}$$

where $\mathbf{F}_{ij}$ is a force acting on the contact area of elastic impacts between the particles i and j. $\mathbf{T}_{i,contact}$ is the summation of torques caused by the contact forces between particles

$$\mathbf{T}_{i,contact} = \sum_{j=1, j \neq i}^{N} \mathbf{T}_{ij} = \sum_{j=1, j \neq i}^{N} \mathbf{d}_{ci} \times \mathbf{F}_{ij} \tag{145}$$

where $\mathbf{d}_{ci}$ is the vector pointing from the centre of gravity of particle i to the contact point with particle j.

The particles of a granular material were spheres of the same material. The simplest linear elastic repulsion and dissipation forces model for normal inter-particle contact forces between two particles i and j was applied.

$$\mathbf{F}_{n,ij} = \mathbf{F}_{n,ij,elastic} + \mathbf{F}_{n,ij,viscous} \tag{146}$$

$$\mathbf{F}_{n,ij,elastic} = k_n R_{ij} h_{ij} \mathbf{n}_{ij} \tag{147}$$

$$\mathbf{F}_{n,ij,viscous} = -\gamma_n m_{ij} \mathbf{v}_{n,ij} \tag{148}$$

where k_n is the spring stiffness coefficient related to Young's modulus, γ_n is the normal dissipation coefficient and m_{ij} is the reduced mass of the contacting particles i and j

$$m_{ij} = \frac{m_i m_j}{m_i + m_j} \tag{149}$$

R_{ij} is the equivalent radius

$$R_{ij} = \frac{R_i R_j}{R_i + R_j} \tag{150}$$

of particles in contact with the radii R_i and R_j, and h_{ij} is the depth of contact overlap.

The tangential force acting between particles was expressed by the Coulomb criteria

$$\mathbf{F}_{t,ij} = -\mathbf{t}_{ij} \min\left(\gamma_t m_{ij} \left|\mathbf{v}_{t,ij}\right|, \mu \left|\mathbf{F}_{n,ij}\right|\right) \tag{151}$$

with γ_t being the tangential dissipation coefficient and μ closely related to the dynamic friction coefficient.

The solution of the equations (141), (142) and (143) is obtained by a 5th - order Gear predictor-corrector scheme. The time step Δt of the integration was chosen such that the entire contact between the particles is resolved with 70-100 time steps.

VI.2 RESULTS

The possibilities offered by the method to simulate particle motion in general and on a moving grate or in a rotary kiln of a combustion device in particular are demonstrated for the granular material consisting of 500 three-dimensional spherical particles of different sizes but of the same material properties, of which the relevant details are listed below

Particle radius	R	0.03 - 0.05	m
Initial velocity	v	0 - 1	m/s
Density	ρ	1000	kg/m^3
Normal spring stiffness coefficient	k_n	$5.0 \cdot 10^5$	Pa
Normal energy dissipation coefficient	γ_n	100	1/s
Tangential energy dissipation coefficient	γ_t	20	1/s
Friction coefficient	μ	100	

Table 2. Particle data

VI.2.1 Packed Bed

Since the initial conditions for particles moving or resting in a packed bed cannot be specified a priori, the calculations were carried out in two stages. Especially since the packaging of the particles results from their previous dynamics, plausible initial conditions can only be obtained by a separate calculation. The first calculation was started with the setup shown in Figure 21 and Figure 22.

Initially, the three-dimensional particles were distributed on an orthogonal and uniform grid represented by a two-dimensional box of 2×3 m in size (Figure 22). The size of the grid cells was equal to the diameter of the largest particle. Thus, particles placed in the centre of the cells did not experience contact with their neighbours. Particle size and initial velocities of the individual particles were chosen randomly. The components of the velocity and the position into the y-direction were set to zero, which limits the motion to the xz-plane. The subsequent motion of particles was calculated taking into account the influence of gravity forces ($g_x = 10$ m/s^2, $g_y = g_z = 0$) and particle contacts occurring during motion. The final result shows how the particles came to rest within a particular arrangement (Figure 23).

The random distribution of particles and void space determines the total volume needed for the arrangement. The grey-coloured scale of the particles represents the overall contact forces acting on a particle, which are inhomogeneously distributed in the packed bed. Connections between neighbouring particles with approximately the same load display the typical arc structures of such arrangements. These arcs act as bridge-like structures concentrating loads on a few particles at the base of their "pillars" and thus hinder the motion.

The results obtained from these calculations were taken as initial conditions for the following calculation, which predicts the motion of particles when they are discharged through an open gate into a combustion chamber of 4×3 m in size. In order to simulate this behaviour, the right wall of the box in Figure 23 was displaced by a certain distance at the start of the calculation. A front of moving particles penetrates the open space like an avalanche as shown in Figure 24.

Once the gate opens, the particles accumulated just behind it discharge into the combustion chamber, moving freely under the effect of gravity forces. While a liquid is subject to the linear variation of the pressure as a function of the depth, the moving bed experiences an inhomogeneous load distribution during the entire motion. During the motion of the bed, the particles order themselves into structures with the contact between them in the bed being more or less strong. These structures are shown in Figure 24 and Figure 25 and indicated by the different gray shades. If particles experiencing approximately the same load were connected by imaginary lines, these would delimit the structures. They extend throughout the bed and in some cases reaching its upper surface. Figure 25 displays the state of the calculation when the front reaches the opposite wall, from where the particles bounce back, some of them leaving the formation completely.

In general, particles in this region have a very loose contact with their neighbours, resembling a fluidised bed to a certain extent. As a result, the void space has increased as compared to a packed arrangement. Again, branches of tree-like structures for the distribution of particles with approximately the same load become apparent and remain throughout the entire motion.
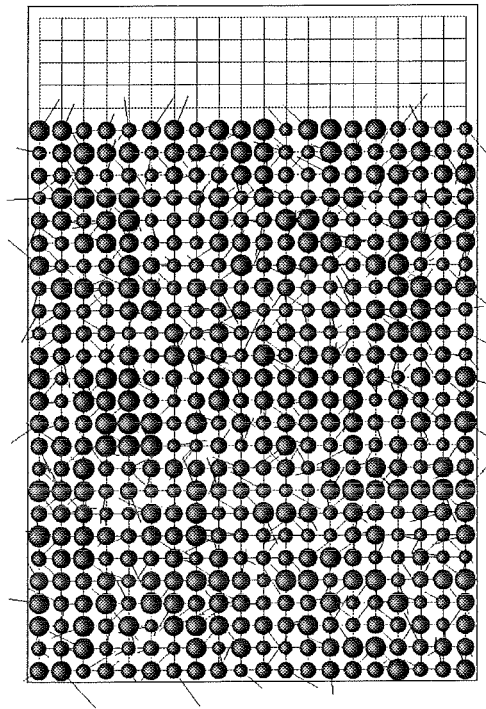
Figure 21. Setup for particle motion
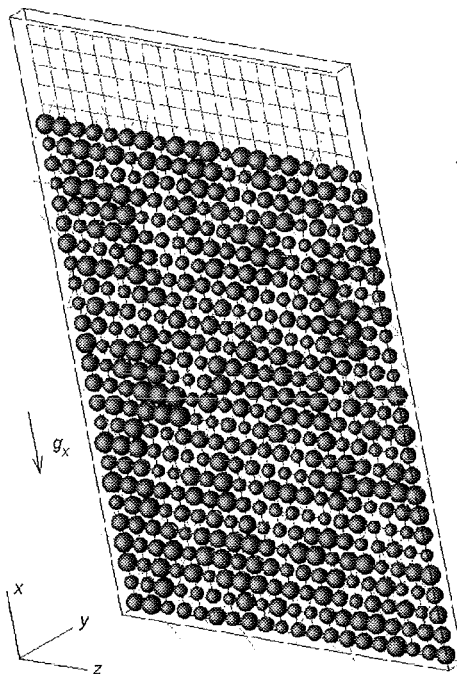
Figure 22. Setup for particle motion: 2D problem in pseudo 3D plane
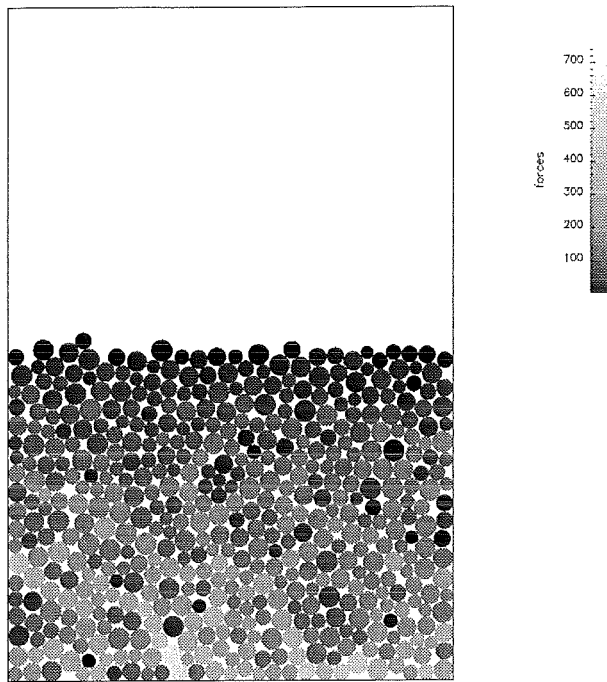
Figure 23. Particles at rest
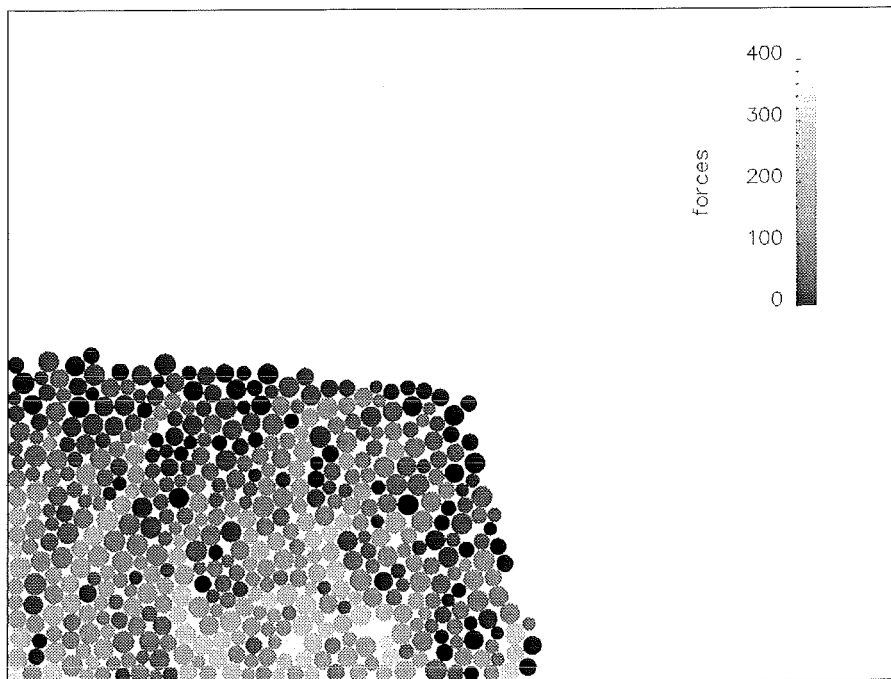
Figure 24. Start of Discharge of particles
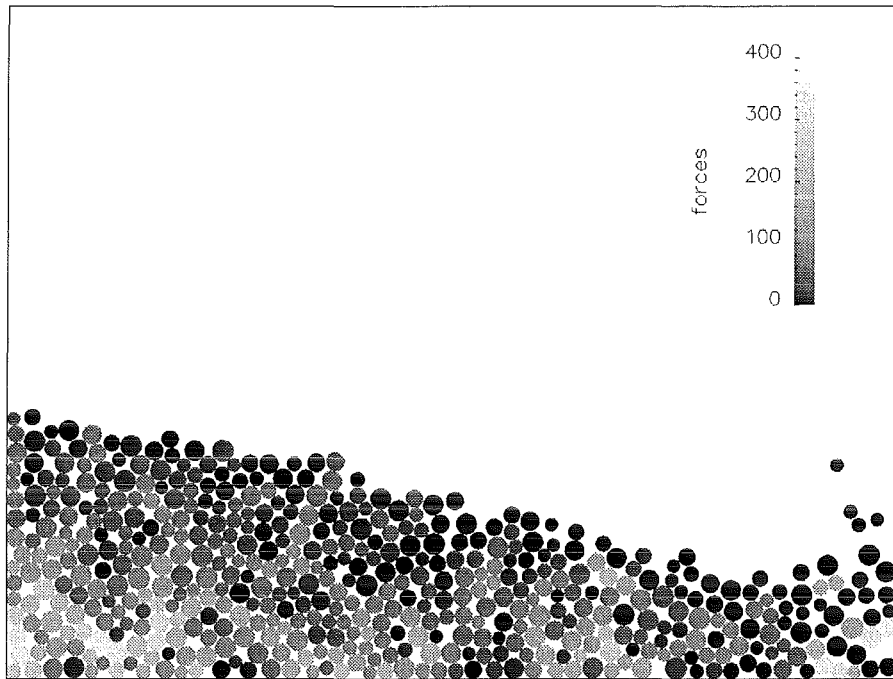
Figure 25. Discharge of particles

VI.2.2 Rotary Kiln

The following example depicts the mixing of granular material in a rotary kiln. Initially, the three-dimensional particles were randomly distributed on a two-dimensional grid formed as a drum of 1.5 m radius without rotation. Under the influence of gravity the particles came to rest after 2 seconds and then the drum started to rotate with angular an angular velocity $w_y = 1$ s^{-1}.

Avalanches occurring during the mixing process form rather flat surfaces of granular material (Figure 26). However, the flow of particles may also form wave-like irregularities on the surface of the granular material (Figure 27), which depend on the inner structure of the granular material and distribution of the contact force.
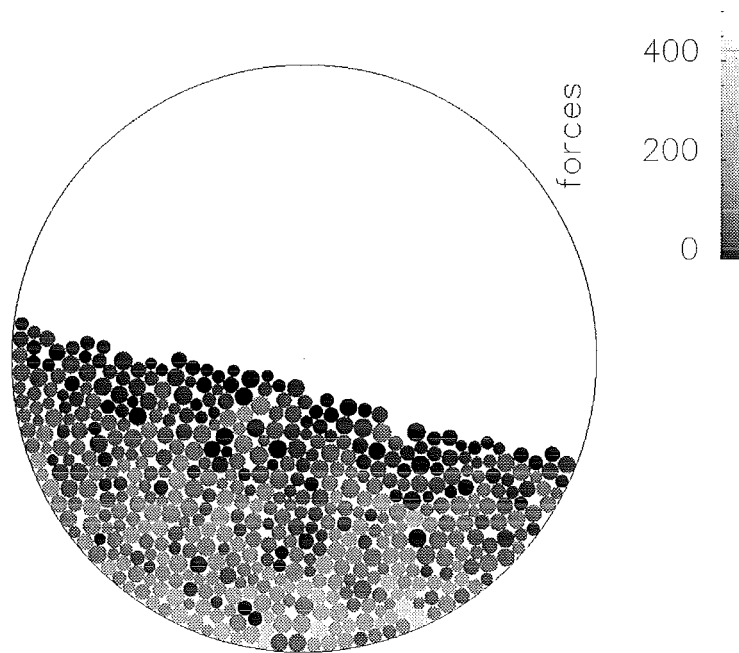
Figure 26. Particles in rotary kiln - almost flat surface of the granular material
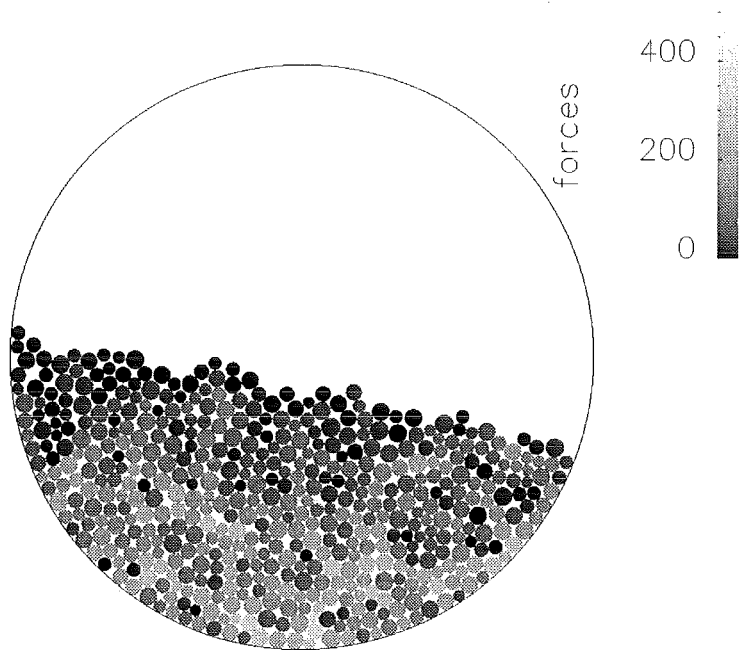
Figure 27. Particles in rotary kiln - waves on the surface of the granular material

VII. CONCLUSIONS:

The objective of this study was to describe a method for the motion of waste material in furnaces, to be used as a module to simulate the entire process of waste combustion. Therefore, an extended literature survey on numerical methods was carried out in order to summarise methods well suited to simulate the behaviour and the motion of granular material. The major methods are represented by the discrete element and the continuum mechanics approach. Furthermore, the interaction between particles during collisions was addressed within the discrete element approach. In the last chapter the equations to describe the motion and the contact between particles in conjunction with their numerical treatment were derived.

Finally, the discrete element approach was implemented in conjunction with the time driven method. The object-oriented technique was chosen to develop the appropriate software module. It was used to calculate several test cases for a packed bed and a rotary kiln. The results show that the method is well suited to simulate the motion of granular material on moving grates and in rotary kilns. Further applications such as in the food processing industry or the industry dealing with solid particles in various kinds are conceivable.

VIII. LIST OF FIGURES

IX. LIST OF TABLES

X. REFERENCES

1. Abu-Zaid S., G. Ahmadi (1993). Analysis of rapid shear flows of granular materials by a kinetic model including frictional losses, Powder Technology, vol.77, pp. 7-17.

2. Adams M.J., B.J. Briscoe (1993). Deterministic micromechanical modelling of failure or flow in discrete planes of densely packed particle assemblies: introductory principles, in Granular Matter, ed. by A. Mechta, Springer-Verlag, pp. 259-291.

3. Akiyama T., K.M. Aoki, T. Iguchi, K. Nishimoto (1996). A fractal properties of vertical vibrated beds of granules, Chemical Engineering Science, vol.51, No.13, pp. 3551-3553.

4. Allen M.P., D. Frenkel, J. Talbot (1989). Molecular dynamics simulation using hard particles, Computer Physics Reports, vol.9, pp. 301-353.

5. Allen M.P., D.J. Tildesley (1990). Computer simulation of liquids, Oxford Science Publication.

6. Aoki K.M., T. Akiyama (1995). Simulation studies of pressure and density wave propagations in vertically vibrated beds of granules, Physical Review E, vol.52, No.3, pp. 3288-3291.

7. Ariel P.D. (1997). Generalized Gear's method for computing the flow of a viscoelastic fluid, Computer Methods in Applied Mechanics and Engineering, vol.142, pp. 111-121.

8. Baekdal L., W. Joosen, T. Larsen, J. Kolafa, J.H. Ovensen, J.W. Parram, H.G. Petersen, R. Bywater, M. Ratner (1997). The objected-oriented development of parallel application in protein dynamics: why we need software tools for HPCN applications, Computer Physics Communications, vol.97, pp. 124-135.

9. Barker G.C. (1993). Computer simulations of granular materials, in Granular Matter, ed. by A. Mechta, Springer-Verlag, pp. 35-83.

10. Barojas J., D. Levesque, B. Quentrec (1973). Simulation of diatomic homonuclear liquids, Physical Review A, vol.7, No.3, pp. 1092-1105.

11. Baxter G.W., R.P. Behringer (1990). Cellular automata models of granular flow, Physical Review A, vol.42, No.2, pp. 1017-1020.

12. Behringer R.P., G.W. Baxter (1993). Pattern formation and complexity in granular flows, in Granular Matter, ed. by A. Mechta, Springer-Verlag, pp. 85-119.

13. Borja R.I., J.R. Wren (1995). Micromechanics of granular media. Part I: Generation of overall constitutive equation for assemblies of circular disks, Computer Methods in Applied Mechanics and Engineering, vol.127, pp. 13-36.

14. Brach R.M. (1984). Friction, restitution and energy loss in planar collisions, Journal of Applied Mechanics, vol.51, pp. 164-170.

15. Brach R.M. (1989). Rigid body collisions, Journal of Applied Mechanics, vol.56, pp. 133-138.

16. Bridgwater J. (1993). Mixing and segregation mechanisms in particle flow, in Granular Matter, ed. by A. Mechta, Springer-Verlag, pp. 161-193.

17. Buchholtz V., T. Poschel (1993). A vectorized algorithm for molecular dynamics of short range interacting particles, International Journal of Modern Physics C, vol.4, No.5, pp. 1049-1057.

18. Buchholtz V., T. Poschel (1994). Numerical investigations of the evolution of sandpiles, Physica A, vol.202, pp. 390-401.

19. Camp P.J., M.P. Allen (1996). Hard ellipsoid rod-plate mixtures: Onsager theory and computer simulation, Physica A, vol.229, pp. 410-427.

20. Campbell C.S. (1990). Rapid granular flows, Annu. Rev. Fluid Mech., vol.22, pp. 57-92.

21. Campbell C.S., C.E. Brennen (1985). Computer simulation of granular shear flows, Journal of Fluid Mechanics, vol.151, pp. 167-188.

22. Cantelaube F., Y. Limon-Duparcmeur, D. Bideau, G.H. Ristow (1995). Geometrical analysis of avalanches in a 2D drum, J. Phys. I France, vol.5, pp. 581-596.

23. Caram H., D.C. Hong (1991). Random-walk approach to granular flows, Physical Review Letters, vol.67, No.7, pp. 828-831.

24. Chang C.S., A. Misra, J.H. Xue (1989). Incremental stress-strain relationships for regular packings made of multi-sized particles, Int.J.Solids Structures, vol.25, No.6, pp. 665-681.

25. Ciccotti G. (1987). in Simulation of liquids and solids, 1987, ed. by G. Ciccoti, D. Frenkel, I.R. McDonald, North-Holland, pp. 325-329.

26. Ciccotti G., M. Ferrario, J.-P. Ryckaert (1982). Molecular dynamics of rigid systems in cartesian coordinates. A general formulation, in Simulation of liquids and solids, 1987, ed. by G. Ciccoti, D. Frenkel, I.R. McDonald, North-Holland, pp. 355-366.

27. Cundall P.A., O.D.L. Strack (1979). A discrete numerical model for granular assemblies, Geotechnique, vol.29, No.1, pp. 47-65.

28. Darmofal D.L., R. Haimes (1996). An analysis of 3D particle path integration algorithms, Journal of Computational Physics, vol.123, pp. 182-195.

29. Derjaguin B.V., V.M. Muller, Yu.P. Toporov (1975). Effect of contact deformations on the adhesion of particles, Journal of Colloid and Interface Science, vol.53, No.2, pp. 314-325.

30. Devillard P. (1990). Scaling behaviour in size segregation ("Brazil Nuts"), J. Phys. I France, vol.51, pp. 369-373.

31. Din X.-D., E. Michaelides (1997). Kinetic theory and molecular dynamics simulations of microscopic flows, Physics of Fluids, vol.9, No.12, pp. 3915-3925.

32. Dury C.M., G.H. Ristow (1997). Radial segregation in a two-dimensional rotating drum, J. Phys. I France, vol.7, pp. 737-745.

33. Ennis B.J., J. Green, R. Davies (1994). The legacy of neglect in the U.S., Chemical Engineering Progress, vol.90, No.32 April, pp. 32-43.

34. Evans D.J. (1977). On the presentation of orientation space, Molecular Physics, vol.34, No.2, pp. 317-325.

35. Evans D.J., S. Murad (1977). Singularity free algorithm for molecular dynamics simulation of rigid polyatomics, in Simulation of liquids and solids, 1987, ed. by G. Ciccoti, D. Frenkel, I.R. McDonald, North-Holland, pp. 367-371.

36. Fan F.-G., G. Ahmadi (1995). Dispersion of ellipsoidal particles in a isotropic pseudo-turbulent flow field, ASME Journals of Fluids Engineering, vol.117, pp. 154-161.

37. Fan L.-S., J. Rathman, A. Ghosh-Dastidar, A.W. Weimer, S. Kimura (1994). The potential of reaction engineering, Chemical Engineering Progress, vol.90, No.32 April, pp. 55-64.

38. Fincham D., M.D. Heyes (1985). Recent advances in molecular-dynamics computer simulation, in Dynamic Proceeses in Codenced Matter - Advances in Chemical Physics. Vol. LXIII, vol.63, ed. by M.W. Evans, John Wiley & Sons, pp. 493-575.

39. Fineberg J. (1996). Physics in a jumping sandbox, Nature, vol.382, No.29 August, pp. 763-764.

40. Form W., N. Ito, G.A. Kohring (1993). Vectorized and parallelized algorithms for multi-million particle MD-simulation, International Journal of Modern Physics C, vol.4, No.6, pp. 1085-1101.

41. Fryer Y.D., C. Bailey, M. Cross, C,-H. Lai (1991). A control volume procedure for solving the elastic stress-strain equations on a structured mesh, Applied Mathematical Modelling, vol.15, pp. 639-645.

42. Gallas J.A.C., H.J. Herrmann, S. Sokolowski (1992). Convection cells in vibrating granular media, Physical Review Letters, vol.69, No.9, pp. 1371-1374.

43. Gallas J.A.C., S. Sokolowski (1993). Grain non-sphericity effects on the angle of repose of granular material, International Journal of Modern Physics B, vol.7, No.9 & 10, pp. 2037-2046.

44. Gavze E., M. Shapiro (1997). Particles in shear flow near a solid wall: effect of nonsphericity on forces and velocities, Int. J. Multiphase Flow, vol.23, No.1, pp. 155-182.

45. Glikman E., I. Kelson, N.V. Doan, H. Tietzet (1996). An optimized algorithm for molecular dynamics simulation of large-scale systems, Journal of Computational Physics, vol.124, pp. 85-92.

46. Goldstein H. (1980). Classical Mechanics, Addison-Wesley Publishing Company.

47. Greenwood J.A., K.L. Johnson (1981). The mechanics of adhesion of viscoelastic solids, Philosophical Magazine, vol.43, No.3, pp. 697-711.

48. Grest G.S., B. Dunweg, K. Kremer (1989). Vectorized link cell Fortran code for molecular dynamics simulations for large number of particles, Computer Physics Communications, vol.55, pp. 269-285.

49. Gu Z.H., P.C. Arnold, A.G. McLean (1992). Prediction of the flow rate of bulk solids from mass flow bins with conical hoppers, Powder Technology, vol.72, pp. 157-166.

50. Haff P., R.S. Anderson (1993). Grain scale simulations of loose sedimentary beds: the example of grain-bed impacts in aeolian saltation, Sedimentology, vol.40, pp. 175-198.

51. Haff P.K. (1993). Discrete mechanics, in Granular Matter, ed. by A. Mechta, Springer-Verlag, pp. 141-160.

52. Haff P.K., B.T. Werner (1986). Computer simulation of the mechanical sorting of grains, Powder Technology, vol.48, pp. 239-245.

53. Herrmann H. (1997). Grains of understanding, Physics World, No.November, pp. 31-34.

54. Hogue C., D. Newland (1994). Efficient computer computation of moving granular particles, Powder Technology, vol.78, pp. 51-66.

55. Hoomans B.P.B., J.A.M. Kuipers, W.J. Briels, W.P.M. Van Swaiij (1996). Discrete particle simulation of bubble and slug formation in a two-dimensional gas-fluidized bed: a hard-sphere approach, Chemical Engineering Science, vol.51, No.1, pp. 99-118.

56. Hopkins M.A. (1992). Numerical Simulation of Systems of Multitudinous Polygonal Blocks, USARREL Report CR 99-22, US Army Cold Regions Research and Engineering Laboratory.

57. Hughes P.C. (1986). Spacecraft Attitude Dynamics, John Wiley & Sons.

58. Jaeger H.M., C. Liu, S.R. Nagel (1989). Relaxation at the angle of response, Physical Review Letters, vol.62, No.1, pp. 40-43.

59. Jaeger H.M., S.R. Nagel (1992). Physics of the granular state, Science, vol.255, pp. 1523-1531.

60. Jaeger H.M., S.R. Nagel (1997). Dynamics of granular material, American Scientist, vol.85, pp. 540-545.

61. Jaeger H.M., S.R. Nagel, R.P. Behringer (1996). The physics of granular materials, Physics Today, No.4, pp. 32-38.

62. Johnson K.L., K. Kendall, A.D. Roberts (1971). Surface energy and the contact of elastic solids, Proc. R. Soc. Lond. A, vol.324, pp. 301-313.

63. Johnson P.C., R. Jackson (1987). Frictional-collisional constitutive relations for granular materials, with application relations to plane shearing, Journal of Fluid Mechanics, vol.176, pp. 67-93.

64. Jullien R., P. Meankin (1987). Simple three dimensional models for ballistic deposition with restructuring, Europhys. Lett, vol.4, No.12, pp. 1385-1390.

65. Kalthoff W., S. Schwarzer, G.H. Ristow, G.J. Herrmann (1996). On hydrodynamic diffusion and velocity fluctuations in two-dimensional simulations of sedimentation, Phys. Fluids, vol.(submitted).

66. Keller J.B. (1986). Impact with friction, Journal of Applied Mechanics, vol.53, pp. 1-4.

67. Khakhar D.V., J.J. McCarthy, J.M. Ottino (1997). Radial segregation of granular mixtures in rotating cylinders, Physics of Fluids, vol.9, No.12, pp. 3600-3614.

68. Khan M.I., G.I. Tardos (1997). Stability of wet agglomerates in granular shear flows, Journal of Fluid Mechanics, vol.347, pp. 347-368.

69. Knowlton T.M., J.W. Carson, G.E. Klinzing, W.-C. Yang (1994). The importance of storage, transfer, and collection, Chemical Engineering Progress, vol.90, No.32 April, pp. 44-54.

70. Kohring G.A. (1993). Computer simulations of sintering via granular dynamics, Physica A, vol.195, pp. 1-11.

71. Kohring G.A. (1994). Computer simulations of granular materials: the effects of mesoscopic forces, J. Phys. I France, vol.4, pp. 1779-1782.

72. Kohring G.A. (1995). Studies of diffusional mixing in rotating drums via computer simulations, J. Phys. I France, vol.5, pp. 1551-1561.

73. Kohring G.A. (1996). Dynamical simulations of granular flows on multi-processor computers, in Computational Methods in Applied Sciences '96, John Wiley & Sons Ltd., pp. 190-196.

74. Kohring G.A. (1996b). A brief technical documentation of the DESim software version 1.2.

75. Kohring G.A., S. Melin, H. Puhl, H.J. Tillemans, W. Vermohlen (1995). Computer simulations of critical, non-stationary granular flow through a hopper, Computer Methods in Applied Mechanics and Engineering, vol.124, pp. 273-281.

76. Kopf A., W. Paul, B. Dunweg (1997). Multiple time step intergrators and momentum conservation, Computer Physics Communications, vol.101, pp. 1-8.

77. Kornilovsky A.N., D.R. Kingdom, A.A. Harms (1996). Pellet dynamics of fuel pellets in suspension, Ann. Nucl. Energy, vol.23, No.3, pp. 171-182.

78. Kumaran V. (1997). Velocity distribution function for a dilute granular material in shear flow, Journal of Fluid Mechanics, vol.340, pp. 319-341.

79. Kuwabara G., K. Kono (1987). Restitution coefficient in a collision between two spheres, Jpn.J.Appl.Phys., vol.26, No.8, pp. 1230-1233.

80. Lan Y., A.D. Rosato (1997). Convection related phenomena in granular dynamics simulations of vibrated beds, Physics of Fluids, vol.9, No.12, pp. 3615-3624.

81. Landau L.D., E.M. Lifshitz (1959). Theory of elasticity. Volume 7 of Course of Theoretical Physics, Pergamon Press.

82. Landau L.D., E.M. Lifshitz (1960). Mechanics. Volume 1 of Course of Theoretical Physics, Pergamon Press.

83. Langston P.A., U. Tuzun, D.M. Heyes (1994). Continuous potential discrete particle simulations of stress and velocity fields in hoppers: transition from fluid to granular flow, Chemical Engineering Science, vol.49, No.8, pp. 1259-1275.

84. Langston P.A., U. Tuzun, D.M. Heyes (1995). Discrete element simulation for granular flow in 2D and 3D hoppers: dependence of discharge rate and wall stress on particle interactions, Chemical Engineering Science, vol.50, No.6, pp. 967-987.

85. Langston P.A., U. Tuzun, D.M. Heyes (1995b). Discrete element simulation of internal stress and flow fields in funnel flow hoppers, Powder Technology, vol.85, pp. 153-169.

86. Langston P.A., U. Tuzun, D.M. Heyes (1996). Distinct element simulation of interstitial air effects in axially symmetric granular flows in hoppers, Chemical Engineering Science, vol.51, No.6, pp. 873-891.

87. Lee J., H.J. Herrmann (1993). Angle of repose and angle of marginal stability: molecular dynamics of granular particles, J. Phys A, vol.26, pp. 373-383.

88. Levesque D., J.-J. Weis, D.W. Oxtoby (1983). A molecular dynamics simulation of rotational and vibrational relaxation in liquid HCl, J.Chem.Phys., vol.79, No.2, pp. 917-925.

89. Lin X., T.-T. Ng (1995). Contact detection algorithms for three-dimensional ellipsoids in discrete element modelling, International Journal for Numerical and Analytical Methods in Geomechanics, vol.19, pp. 653-659.

90. Lin X., T.-T. Ng (1997). A three-dimensional discrete element model using arrays of ellipsoids, Geotechnique, vol.47, No.2, pp. 319-329.

91. Lubachevsky B.D. (1991). How to simulate billiards and similar systems, Journal of Computational Physics, vol.94, pp. 255-283.

92. Lubachevsky B.D., V. Privman, S.C. Roy (1996). Casting pearls ballistically: efficient massively parallel simulation of particle deposition, Journal of Computational Physics, vol.126, pp. 152-164.

93. Lubkin G.B. (1997). Experiments find hysteresis and precursors in the stick-flip friction of a granular system, Physics Today, No.September, pp. 17-19.

94. Luding S., E. Clement, A. Blumen, J. Rajchenbach, J. Duran (1994). Anomalous energy dissipation in molecular-dynamics simulations of grains: The "detachment" effect, Physical Review E, vol.50, No.5, pp. 4113-4122.

95. Luding S., J. Duran, E. Clement, J. Rajchenbach (1996). Simulation of dense granular flow: dynamic arches and spin organization, J. Phys. I France, vol.6, pp. 823-836.

96. Maeno Y. (1996). Numerical investigation of surface level instability due to a tube in vibrating bed of powder, Physica A, vol.232, pp. 27-39.

97. Makino J., M. Taiji, T. Ebisuzaki, D. Sugimoto (1994). GRAPE-4: A one Tflops special purpose computer for astrophysical N-body problem, in Proceedings of the conference on Supercomputing'94, November 1994, pp. 429-438.

98. Marin M. (1997). Event-driven hard-particle molecular dynamics using bulk-synchronous parallelism, Computer Physics Communications, vol.102, pp. 81-96.

99. McNamara S., W.R. Young (1994). Inelastic collapse in two dimensions, Physical Review E, vol.50, No.1, pp. R28-R31.

100. McNamara S., W.R. Young (1996). Dynamics of a freely evolving, two-dimensional granular medium, Physical Review E, vol.53, No.5, pp. 5089-5100.

101. Meankin P., R. Jullien (1992). Simple model for two and three dimensional particle size segregation, Physica A, vol.180, pp. 1-18.

102. Metcalfe G., T. Shinbrot, J.J. McCarthy (1995). Avalanche mixing of granular solids, Nature, vol.374, No.2, pp. 39-41.

103. Mindlin R.D. (1949). Compliance of Elastic Bodies in Contact, J.Appl.Mech.Trans.ASME, vol.16, pp. 259-268.

104. Mindlin R.D., H. Deresiewicz (1953). Elastic spheres in contact under varying oblique forces, J.Appl.Mech.Trans.ASME, vol.20, pp. 327-344.

105. Nasuno S., A. Kudrolli, J.P. Gollub (1997). Friction in granular layers: hysteresis and precursors, Physical Review Letters, vol.79, No.5, pp. 949-952.

106. Nederman R.M. (1992). Statics and kinematics of granular material, Cambridge University Press.

107. Newmark N.M., F. Asce (1959). A method of computation for structural dynamics, J.Engng.Mech.Div.Proc.ASCE (EM3), vol.85, pp. 67-94.

108. Nolan G.T., P.E. Kavanagh (1995). Random packing of nonspherical particles, Powder Technology, vol.84, pp. 199-205.

109. Oakeshott R.B.S., S.F. Edvards (1994). Pertubative theory of the packing of mixtures and of non-spherical particles, Physica A, vol.202, pp. 482-498.

110. Ovensen J.H., H.G. Petersen, J.W. Perram (1996). Comparison of two methods for solving linear equations occuring in molecular dynamics applications, Computer Physics Communications, vol.94, pp. 1-18.

111. Penna G.L., V. Minicozzi, S. Morante, G.C. Rossi, G. Salina (1997). Molecular dynamics with massively parallel APE computers, Computer Physics Communications, vol.106, pp. 53-68.

112. Perram J.W., M.S. Wertheim (1985). Statistical mechanics of hard ellipsoids. I. Overlap algorithm and the contact function, Journal of Computational Physics, vol.58, pp. 409-416.

113. Perram J.W., M.S. Wertheim, J.L. Lebowitz, G.O. Williams (1984). Monte Carlo simulations of hard spheroids, Chemical Physics Letters, vol.105, No.3, pp. 277-280.

114. Peters B. (1997).Numerical Simulation of Packed Bed Combustion, In 4th European Conference on Industrial Furnaces and Boilers, Porto, Portugal, April 1-4, 1997

115. Peters B. (1996). Efficient software development and use for engineering applications with TOSCA (Tools of Object-oriented Software for Continuum Mechanics Applications), pp 185 -192, In CFD 96, Fourth Annual Conference of the CFD Society of Canada, Ottawa, Ontario, Canada, June 2-4, 1996.

116. Peters B. (1997). Application de la conception object oriente a la modelisation de l'incineration de dechets municipaux, pp 668 - 677, In Informatique pour l'Environnement'97, Conference Europeenne sur les Technologies de l'Information pour l'Environnement, 10-12 Septembre 1997, Strasbourg.

117. Peters M.H. (1994). Nonequilibrium molecular dynamics simulation of free-molecule gas flows in complex geometries with application to Brownian motion of aggregate aerosols, Physical Review E, vol.50, No.6, pp. 4609-4617.

118. Plimpton S. (1995). Fast parallel algorithms for short-range molecular dynamics, Journal of Computational Physics, vol.117, pp. 1-19.

119. Polderman H.G., J. Boom, E. De Hilster, A.M. Scott (1987). Solids flow velocity profiles in mass flow hoppers, Chemical Engineering Science, vol.42, No.4, pp. 737-744.

120. Poschel T., V. Buchholtz (1993). Static friction phenomena in granular materials: Coulomb law versus particle geometry, Physical Review Letters, vol.70, No.24, pp. 3963-3966.

121. Potapov A.V., C.S. Campbell, M.A. Hopkins (1995). A two dimensional dynamic solution of solid fracture. Part II: Examples, International Journal of Modern Physics C, vol.6, No.3, pp. 399-425.

122. Potapov A.V., M.A. Hopkins, C.S. Campbell (1995). A two dimensional dynamic solution of solid fracture. Part I: Description of model, International Journal of Modern Physics C, vol.6, No.3, pp. 371-398.

123. Quwerkerk C.E.D. (1991). A micro-mechanical connection between the single-particle strength and the bulk strength of random packings of spherical particles, Powder Technology, vol.65, pp. 125-138.

124. Rahman A., F.H. Stillinger (1971). Molecular dynamics study of liquid water, in Simulation of liquids and solids, 1987, ed. by G. Ciccoti, D. Frenkel, I.R. McDonald, North-Holland, pp. 330-353.

125. Rapaport D.C. (1980). The event scheduling problem in molecular dynamic simulation, Journal of Computational Physics, vol.34, pp. 184-201.

126. Rapaport D.C. (1988). Large-scale molecular dynamics simulation using vector and parallel computers, Comp. Phys. Rep., vol.9, pp. 1-53.

127. Rapaport D.C. (1991). Multi-million particle molecular dynamics: I. Design considerations for vector processing, Computer Physics Communications, vol.62, pp. 198-216.

128. Rapaport D.C. (1991b). Multi-million particle molecular dynamics: II. Design considerations for distributed processing, Computer Physics Communications, vol.62, pp. 217-228.

129. Rapaport D.C. (1993). Multi-million particle molecular dynamics: III. Design considerations for data parallel processing, Computer Physics Communications, vol.76, pp. 301-317.

130. Reynders V.W., D.W. Forslund, P.J. Hinker, M. Tholburn, D.G. Kilman, W.F. Humhprey (1995). OOPS: an object-oriented particle simulation class library for distributed architectures, Computer Physics Communications, vol.87, pp. 212-224.

131. Rietema K. (1991). The Dynamics of Fine Powders, Elsevier Applied Science, London.

132. Ristow G.H. (1992). Simulating granular flow with molecular dynamics, J. Phys. I France, vol.2, pp. 649-662.

133. Ristow G.H. (1992b). Molecular dynamics simulations of granular materials on the Intel iPSC/860, International Journal of Modern Physics C, vol.3, No.6, pp. 1281-1293.

134. Ristow G.H. (1994b). Granular dynamics: a review about recent molecular dynamics simulations of granular materials, Annual Reviews of Computational Physics I, ed. by D. Stauffer, World Scientific, Singapore, pp. 275-308.

135. Ristow G.H. (1996b). Dynamics of granular materials in a rotating drum, Europhys. Lett, vol.34, No.4, pp. 263-268.

136. Ristow G.H., G. Strassburger, I. Rehberg (1997). Phase diagram and scaling of granular materials under horizontal vibrations, Physical Review Letters, vol.79, No.5, pp. 833-836.

137. Ristow G.H., H.J. Herrmann (1994c). Forces on the walls and stagnation zones in a hopper filled with granular material, Physica A, vol.213, pp. 474-481.

138. Rosato A., K.J. Strandburg, F. Prinz, R.H. Swendsen (1987). Why the Brazil Nuts are on top: size segregation of particulate matter by shaking, Physical Review Letters, vol.58, No.10, pp. 1038-1040.

139. Rothenburg L., R.J. Bathurst (1991). Numerical simulation of idealized granular assemblies with plane elliptical particles, Computers and Geotechnics, vol.11, pp. 315-329.

140. Runesson K., L. Nilsson (1986). Finite element modelling of the gravitational flow of a granular material, Bulk solids, vol.6, No.5, pp. 877-884.

141. Sadd M.H., A. Shukla, H. Mei (1989). Computational and experimental modeling of wave propagation in granular materials, Proc. 4th Int. Conf. Computational Methods and Experimental Measurements, pp. 325-334.

142. Sadd M.H., Q. Tai, A. Shukla (1993). Contact law effects on wave propagation in particulate materials using distinct element modeling, Int.J.Non-Linear Mech., vol.28, No.2, pp. 251-265.

143. Satoh A. (1995). Molecular dynamics simulations on internal structures of normal shock waves in Lennard-Jones liquids, ASME Journals of Fluids Engineering, vol.117, pp. 97-103.

144. Satoh A. (1995b). Stability of computational algorithms used in molecular dynamics simulations, ASME Journals of Fluids Engineering, vol.117, pp. 531-534.

145. Satoh A. (1997). Stability of various molecular dynamics algorithms, ASME Journals of Fluids Engineering, vol.119, pp. 476-480.

146. Savage S.B. (1988). Streaming motions in a bed of vibrationally fluidized dry granular material, Journal of Fluid Mechanics, vol.194, pp. 457-478.

147. Shida K., R. Suzuki, T. Kawai (1997). Numerical error of total energy: Dependence on time step, Computer Physics Communications, vol.102, pp. 59-67.

148. Shinbrot T. (1997). Competition between randomizing impacts and inelastic collisions in granular pattern formation, Nature, vol.389, No.9 October, pp. 574-576.

149. Srinivasan S.G., I. Ashok, H. Jonsson, G. Kalonji, J. Zahorjan (1997). Parallel short-range molecular dynamics using the Adhara runtime system, Computer Physics Communications, vol.102, pp. 28-43.

150. Srinivasan S.G., I. Ashok, H. Jonsson, G. Kalonji, J. Zahorjan (1997b). Dynamics-domain-decomposition parallel molecular dynamics, Computer Physics Communications, vol.102, pp. 44-58.

151. Stovall T., F. De Larrard, M. Buil (1986). Linear packing density model of grain mixtures, Powder Technology, vol.48, pp. 1-12.

152. Stronge W.J. (1990). Rigid body collision with friction, Proc. R. Soc. Lond. A, vol.431, pp. 169-181.

153. Stroustrup B. (1991). The C++ Programming Language, Addison-Wesley Publishing Company.

154. Sundaram S., L.R. Collins (1996). Numerical considerations in simulating a turbulent suspension of finite-volume particles, Journal of Computational Physics, vol.124, pp. 337-350.

155. Tabor D. (1978). On the role of molecular forces in contact deformations (Critical remarks concerning Dr.Tabor's Report), Journal of Colloid and Interface Science, vol.67, No.2, pp. 380.

156. Taguchi Y-h. (1992). Powder turbulence: direct onset of turbulent flow, J. Phys. II France, vol.2, pp. 2103-2114.

157. Taguchi Y-h. (1992b). New origin of a convective motion: elastically induced convection in granular materials, Physical Review Letters, vol.69, No.9, pp. 1367-1370.

158. Thompson P.A., G.S. Grest (1991). Granular flow: Friction and the dilatancy transition, Physical Review Letters, vol.67, pp. 1751-1754.

159. Thornton C., K.K. Yin (1991). Impact of elastic spheres with and without adhesion, Powder Technology, vol.65, pp. 153-166.

160. Ting J.M. (1991). An ellipse-based micromechanical model for angular granular materials, in Proc.ASCE Engineering Mechanics Conference on Mechanics Computing in 1990' and Beyond, No.Part 2, ed. by Hojjat Adeli, Columbus, OH, pp. 1214-1218.

161. Ting J.M., B.T. Corkum (1992). Computational laboratory for discrete element geomechanics, Journal of Computing in Civil Engineering, vol.6, No.2, pp. 129-146.

162. Ting J.M., M. Khwaja, L. Meachum, J.D. Rowell (1993). An ellipse-based discrete element model for granular materials, International Journal for Numerical and Analytical Methods in Geomechanics, vol.17, pp. 603-623.

163. Tsuji Y., T. Kawaguchi, T. Tanaka (1993). Discrete particle simulation of two-dimensional fluidised bed, Powder Technology, vol.77, pp. 79-87.

164. Tsuji Y., T. Tanaka, T. Ishida (1992). Lagrangian numerical simulation of plug flow of cohesionless particles in a horizontal pipe, Powder Technology, vol.71, pp. 239-250.

165. Umbanhowar P. (1997). Patterns in the sand, Nature, vol.389, No.9 October, pp. 541-542.

166. Umbanhowar P.B., F. Melo, H.L. Swinney (1996). Localized excitations in a vertically vibrated granular layer, Nature, vol.382, No.29 August, pp. 793-796.

167. van Gunsteren W.F., H.J.C. Berendsen (1977). Algorithm for macromolecular dynamics and constraint dynamics, Molecular Physics, vol.34, No.5, pp. 1311-1327.

168. van Gunsteren W.F., H.J.C. Berendsen, F. Colonna, D. Perania, J.P. Hollenberg, D. Lellouch (1984). On searching neighbours in computer simulations of macromolecular systems, Journal of Computational Chemistry, vol.5, No.3, pp. 272-279.

169. Verboncoer J.P., A.B. Langdon, N.T. Glaad (1995). An object-oriented electromagnetic PIC code, Computer Physics Communications, vol.87, pp. 199-211.

170. Verlet L. (1967). Computer "experiments" on classical fluids. I. Thermodynamical properties of Lennard-Jones molecules, in Simulation of liquids and solids, 1987, ed. by G. Ciccoti, D. Frenkel, I.R. McDonald, North-Holland, pp. 68-73.

171. Vimawala M.S., G.M. Turkiyyah (1995). Computational procedures for topological shape design, Computer Methods in Applied Mechanics and Engineering, vol.125, pp. 257-285.

172. Walton O.R., R.L. Braun (1986). Viscosity, granular-temperature, and stress calculations for shearing assemblies of inelastic, frictional disks, Journal of Rheology, vol.30, No.5, pp. 949-980.

173. Wang Y., M.T. Mason (1992). Two-dimensional rigid-body collision with friction, Journal of Applied Mechanics, vol.59, pp. 635-642.

174. Williams J.R., A.P. Pentland (1992). Superquadratics and modal dynamics for discrete elements in interactive design, Engineering Computations, vol.9, pp. 115-127.

175. Williams J.R., R. O'Connor (1995). A linear complexity intersection algorithm for discrete element simulation of arbitrary geometries, Engeneering Computations, vol. 12, pp. 185-201.

176. Wren J.R., R.I. Borja (1997). Micromechanics of granular media. Part II: Overall tangential moduli and localization model for periodic assemblies of circular disks, Computer Methods in Applied Mechanics and Engineering, vol.141, pp. 221-246.

177. Xu B.H., A.B. Yu (1997). Numerical simulation of the gas-solid flow in a fluidized bed by combining discrete particle method with computational fluid dynamics, Chemical Engineering Science, vol.52, No.16, pp. 2785-2809.

178. Yevtushenko A.A., R.D. Kulchytsky-Zhyhailo (1997). Simplified solution for elliptical-contact problem with wear, Int.J.Engng.Sci., vol.35, No.14, pp. 1327-1334.